21. **Liu, T., B. Lu, I. Lee, G. Ondrovicova, E. Kutejova, and C. K. Suzuki.** 2004. DNA and RNA binding by the mitochondrial lon protease is regulated by nucleotide and protein substrate. J. Biol. Chem. **279**:13902–13910.
22. **Matsushima, Y., K. Matsumura, S. Ishii, H. Inagaki, T. Suzuki, Y. Matsuda, K. Beck, and Y. Kitagawa.** 2003. Functional domains of chicken mitochondrial transcription factor A for the maintenance of mitochondrial DNA copy number in lymphoma cell line DT40. J. Biol. Chem. **278**:31149–31158.
23. **McCulloch, V., B. L. Seidel-Rogol, and G. S. Shadel.** 2002. A human mitochondrial transcription factor is related to RNA adenine methyltransferases and binds *S*-adenosylmethionine. Mol. Cell. Biol. **22**:1116–1125.
24. **McCulloch, V., and G. S. Shadel.** 2003. Hum. mitochondrial transcription factor B1 interacts with the C-terminal activation region of h-mtTFA and stimulates transcription independently of its RNA methyltransferase activity. Mol. Cell. Biol. **23**:5816–5824.
25. **Megraw, T. L., and C. B. Chae.** 1993. Functional complementarity between the HMG1-like yeast mitochondrial histone HM and the bacterial histone-like protein HU. J. Biol. Chem. **268**:12758–12763.
26. **Miyakawa, I., N. Sando, S. Kawano, S. Nakamura, and T. Kuroiwa.** 1987. Isolation of morphologically intact mitochondrial nucleoids from the yeast, Saccharomyces cerevisiae. J. Cell Sci. **88**:431–439.
27. **Muta, T., D. Kang, S. Kitajima, T. Fujiwara, and N. Hamasaki.** 1997. p32 protein, a splicing factor 2-associated protein, is localized in mitochondrial matrix and is functionally important in maintaining oxidative phosphorylation. J. Biol. Chem. **272**:24363–24370.
28. **Ohno, T., S. Umeda, N. Hamasaki, and D. Kang.** 2000. Binding of human mitochondrial transcription factor A, an HMG box protein, to a four-way DNA junction. Biochem. Biophys. Res. Commun. **271**:492–498.
29. **Pardue, M. L., J. M. Fostel, and T. R. Cech.** 1984. DNA-protein interactions in the Drosophila virilis mitochondrial chromosome. Nucleic Acids Res. **12**:1991–1999.
30. **Parisi, M. A., B. Xu, and D. A. Clayton.** 1993. A human mitochondrial transcriptional activator can functionally replace a yeast mitochondrial HMG-box protein both in vivo and in vitro. Mol. Cell. Biol. **13**:1951–1961.
31. **Potter, D. A., J. M. Fostel, M. Berninger, M. L. Pardue, and T. R. Cech.** 1980. DNA-protein interactions in the Drosophila melanogaster mitochondrial genome as deduced from trimethylpsoralen crosslinking patterns. Proc. Natl. Acad. Sci. USA **77**:4118–4122.
32. **Sasaki, N., H. Kuroiwa, C. Nishitani, H. Takano, T. Higashiyama, T. Kobayashi, Y. Shirai, A. Sakai, S. Kawano, K. Murakami-Murofushi, and T. Kuroiwa.** 2003. Glom is a novel mitochondrial DNA packaging protein in Physarum polycephalum and causes intense chromatin condensation without suppressing DNA functions. Mol. Biol. Cell **14**:4758–4769.
33. **Seidel-Rogol, B. L., and G. S. Shadel.** 2002. Modulation of mitochondrial transcription in response to mtDNA depletion and repletion in HeLa cells. Nucleic Acids Res. **30**:1929–1934.
34. **Shadel, G. S., and D. A. Clayton.** 1997. Mitochondrial DNA maintenance in vertebrates. Annu. Rev. Biochem. **66**:409–435.
35. **Spelbrink, J. N., F. Y. Li, V. Tiranti, K. Nikali, Q. P. Yuan, M. Tariq, S. Wanrooij, N. Garrido, G. Comi, L. Morandi, L. Santoro, A. Toscano, G. M. Fabrizi, H. Somer, R. Croxen, D. Beeson, J. Poulton, A. Suomalainen, H. T. Jacobs, M. Zeviani, and C. Larsson.** 2001. Hum. mitochondrial DNA deletions associated with mutations in the gene encoding Twinkle, a phage T7 gene 4-like protein localized in mitochondria. Nat. Genet. **28**:223–231.
36. **Takamatsu, C., S. Umeda, T. Ohsato, T. Ohno, Y. Abe, A. Fukuoh, H. Shinagawa, N. Hamasaki, and D. Kang.** 2002. Regulation of mitochondrial D-loops by transcription factor A and single-stranded DNA-binding protein. EMBO Rep. **3**:451–456.
37. **Tang, Y., E. A. Schon, E. Wilichowski, M. E. Vazquez-Memije, E. Davidson, and M. P. King.** 2000. Rearrangements of human mitochondrial DNA (mtDNA): new insights into the regulation of mtDNA copy number and gene expression. Mol. Biol. Cell **11**:1471–1485.
38. **Yang, M. Y., M. Bowmaker, A. Reyes, L. Vergani, P. Angeli, E. Gringeri, H. T. Jacobs, and I. J. Holt.** 2002. Biased incorporation of ribonucleotides on the mitochondrial L-strand accounts for apparent strand-asymmetric DNA replication. Cell **111**:495–505.
39. **Zelenaya-Troitskaya, O., S. M. Newman, K. Okamoto, P. S. Perlman, and R. A. Butow.** 1998. Functions of the high mobility group protein, Abf2p, in mitochondrial DNA segregation, recombination and copy number in Saccharomyces cerevisiae. Genetics **148**:1763–1776.

ANALYTICAL SCIENCES NOVEMBER 2004, VOL. 20

2004 © The Japan Society for Analytical Chemistry

Notes

Mutation Detection in the Drug-Resistant Hepatitis B Virus Polymerase Gene Using Nanostructured Reverse Micelles

Lian-Chun PARK,* Tatsuo MARUYAMA,* Noriho KAMIYA,* Masahiro GOTO,*,† Hiroyuki KUMA,*** and Naotaka HAMASAKI*****

**Department of Applied Chemistry, Graduate School of Engineering, Kyushu University, 6-10-1 Hakozaki, Fukuoka 812-8581, Japan*
***PRESTO, JST (Japan Science and Technology Corporation)*
****Department of Clinical Chemistry and Laboratory Medicine, Graduate School of Medical Sciences, Kyushu University, Fukuoka 812-8582, Japan*

The emergence of drug-resistant hepatitis B virus (HBV) has been reported in patients with prolonged administration of lamivudine, which is a potent drug for the prevention of HBV infection. Lamivudine-resistant HBV has several types of mutations at the YMDD motif of its DNA polymerase. We successfully demonstrated that monitoring the hybridization behavior in nanostructured reverse micelles enables us to detect single nucleotide polymorphisms (SNPs). With the aid of reverse micelles, a model 40-mer oligonucleotide containing a single-base substitution was clearly distinguished from the normal, complementary oligonucleotide. In addition, we extended this technique to a high-throughput analysis. The results obtained with a 96-well micro-plate reader indicated the possibility of SNPs detection toward multiple samples of patients.

(Received August 16, 2004; Accepted September 16, 2004)

Most of the current therapeutic approaches for chronic hepatitis B virus (HBV) infection focus on the RNA-dependent DNA polymerase as a target molecule for inhibiting HBV replication. A new nucleoside analogue, lamivudine [(−) 2′-deoxy-3′-thiacytidine], appears to be a potent inhibitor of the DNA polymerase, and is under clinical use. Although treatments with lamivudine for chronic hepatitis B show a rapid decline of HBV DNA levels in serum, prolonged treatments often result in the emergence of lamivudene-resistant HBV.[1,2] The drug-resistant HBV is associated with mutations in the YMDD motif of the polymerase within the conserved sub-domain C, of which the substitutions of Met552 to either isoleucine (M552I, YIDD variant) or valine (M552V, YVDD variant) have been found.[3] These mutations are mainly identified after several months of lamivudine treatment with a re-elevation of serum HBV DNA and the transaminase levels. The identification of a mutation at the early stage is crucial for an effective treatment, and has thus been carried out either by a nucleotide sequencing or polymerase chain reaction (PCR)-based analyses.[3]

We have recently proposed a promising method for SNPs detection in targeted DNA sequences using reverse micelles with non-labeled DNA by simply monitoring the change in the UV absorbance at 260 nm.[4,5] In the present study, this novel method was applied to detect single-nucleotide substitution within a model 40-mer oligonucleotide corresponding to the mutation found in the YMDD motif upon long-term administration of lamivudine. We additionally tested the applicability of this technique to multi-sample detection with a 96-well micro-plate format.

† To whom correspondence should be addressed.
E-mail: mgototcm@mbox.nc.kyushu-u.ac.jp

Materials and Methods

Reagents

Sodium di-2-ethylhexyl sulfosuccinate (AOT) was obtained from Kishida Chemical Co. (Japan). All other chemicals were obtained from commercial suppliers, and were of the highest purity available. The probe and target oligonucleotides (P1 and T1 - T5, respectively) were designed based on the DNA sequences around the mutation site of the YMDD motif (Table 1). All of the oligonucleotides were obtained from Hokkaido System Science Co. Ltd. (Sapporo, Japan).

Experimental procedures

Each oligonucleotide was dissolved in a 10 mM (1 M = 1 mol dm^{-3}) Tris-HCl buffer (pH 7.0, containing 1 mM EDTA). The concentrations were adjusted to 198 μM by measuring the absorbance at 260 nm. A reverse-micellar solution containing a single-stranded oligonucleotide was prepared by directly injecting 9 μl of the probe aqueous solution (198 μM) into 1 ml of a 50 mM AOT/isooctane solution. The targeted oligonucleotide solution (9 μl) was then injected into the reverse micellar-solution in the same way to initiate DNA hybridization at 15°C. The final W_0 value (*i.e.* the molar ratio of water to AOT in the system: $[H_2O]/[AOT]$) was set to be 20. The apparent concentration of each oligonucleotide was 1.75 μM, based on the total volume. DNA hybridization in reverse micelles was monitored by the absorbance change at 260 nm and 15°C using a UV-vis spectrophotometer (JASCO Vbest-570).

In a high-throughput experiment, a 96-well glass plate was employed for the use of an organic solvent. The glass plate was

Table 1 Oligonucleotide sequences of the targets and the probe tested in this study

Probe	
P1: 3′-ACA AAC CGA AAG TCA ATA TAC CTA CTA CAC CAT AAC CCC C-5′	
Target[a]	
T1: 5′-TGT TTG GCT TTC AGT TAT ATG GAT GAT GTG GTA TTG GGG G-3′	
T2: 5′-TGT TTG GCT TTC AGT TAT **G**TG GAT GAT GTG GTA TTG GGG G-3′	
T3: 5′-TGT TTG GCT TTC AGT TAT ATA GAT GAT GTG GTA TTG GGG G-3′	
T4: 5′-TGT TTG GCT TTC AGT TAT ATT GAT GAT GTG GTA TTG GGG G-3′	
T5: 5′-TGT TTG GCT TTC AGT TAT ATC GAT GAT GTG GTA TTG GGG G-3′	

a. T1 oligonucleotide has the complementary sequence for P1 (YMDD motif of HBV is underlined). The single nucleotide substitutions in T2 to T5 are shown as a bold, underlined character.

specially prepared by Nippon Sheet Glass Co., Ltd. A 100 µl portion of a 50 mM AOT/isooctane solution was filled in the first line of the 96-well micro-plate, then, a 1.0 µl of the P1 oligonucleotide solution was added to the 6 wells in the first line of the glass plate. Furthermore, a target oligonucleotide solution of T1 to T5, listed in Table 1, was added to each well in the same way. The apparent concentration of each oligonucleotide was 2.0 µM, based on the total solution volume, and the water content (W_0) in the reverse micelles was set to be 20. The UV measurement was carried out after thoroughly mixing the solutions in the instrument for 10 min at room temperature (at around 25°C). The decrease in the absorbance at 260 nm was detected with time by a micro-plate reader (Power Wave X: BIO-TEK Instruments INC.).

Data analysis

Following the change in the absorbance at 260 nm with time and data acquisition, the difference in the absorbance between the maximum and the minimum values observed during 1-h of hybridization was normalized by those obtained with a full-matched pair as unity. The relative difference in the absorbance was used to evaluate the mutation detection.

Results and Discussion

Figure 1 is a schematic representation of DNA hybridization in reverse micelles. In reverse micelles, it appeared that DNA hybridization is markedly retarded, which facilitates direct monitoring of that process by simply following the UV absorbance change.[4,5] Based on this new concept, we first investigated DNA hybridization between full-matched (P1 and T1) or mismatched (P1 and T2 - 5) base pairs (Table 1) using a UV-visible spectrophotometer.

Figure 2A shows the time courses of hybridization of P1 with the targets. One can see from the figure that an absorbance change between the full- and the mismatched pairs is evident after 1-h hybridization. The relative changes in the absorbance depicted in Fig. 2B thus clearly shows the potential of reverse micelles to distinguish normal and mutated HBV genes at the level of single nucleotide substitution. It is worth noting that the ability of reverse micelles in discrimination seems to be dependent on the type of mismatched bases. With respect to the

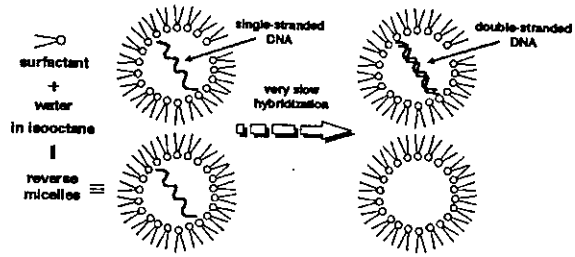

Fig. 1 Schematic illustration of DNA hybridization in reversed micelles.

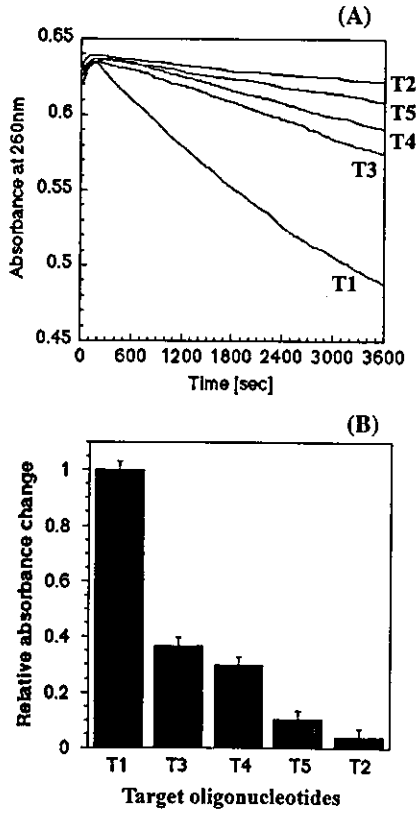

Fig. 2 (A) Time courses of the hybridization of P1 (probe) with full-matched (T1) or mis-matched (T2 - 5) targets using a UV-vis spectrophotometer. (B) Relative changes in the UV absorbance at 260 nm during 1-h incubation. The error bars in the figure represent the standard deviation in triplicate experiments.

single nucleotide substitution at the same position (P1 and T3 - 5), a C-C (P1-T5) mismatch was likely to be unstable, rather than both C-A (P1-T3) and C-T (P1-T4) mismatches (Fig. 2B). Based on a report corresponding the nearest neighbor base pair parameters,[6] the stability of the C-A and C-T mismatches is higher than that of the C-C mismatch. Therefore, the order of the hybridization rates in the five different samples is considered to be reasonable. These results indicate that nanostructured reverse micelles enable us to detect single-base mutations in the YMDD motif without labeling or immobilizing DNA probes, which is usually required for DNA chip technology.

Finally, we extended this new methodology to high-throughput manipulation. For that purpose, we employed a commercially available 96-well micro-plate reader with UV detection. The results are summarized in Fig. 3. Under the

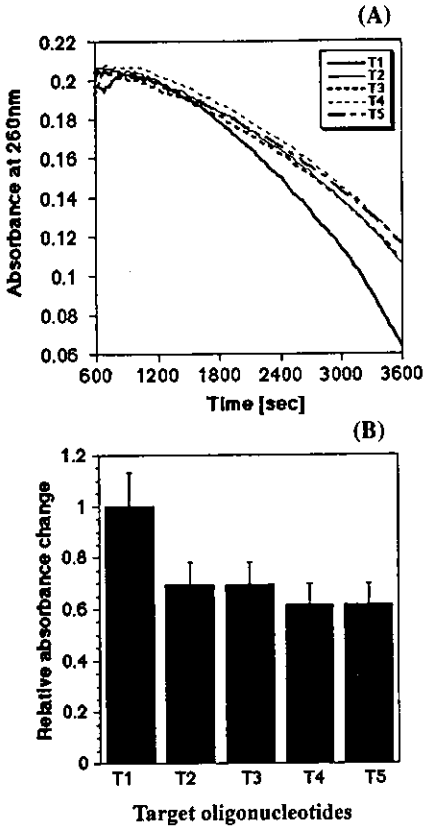

Fig. 3 (A) Time courses of the hybridization of P1 (probe) with full-matched (T1) or mis-matched (T2 - 5) targets using a 96-well micro-plate reader. (B) Relative changes in the UV absorbance at 260 nm during 1-h incubation. The error bars in the figure represent the standard deviation in triplicate experiments.

optimized conditions described in the experimental section, we could detect the difference between the full-matched and the mismatched targets by measuring the absorbance change observed in a 96-well format (Fig. 3A). Although the relative changes in absorbance between the full-matched and mismatched DNAs could be distinguished (Fig. 3B), the discrimination between mismatched targets (T2 - 5) became impossible in contrast to the results in Fig. 2B. It should be noted that the absorbance with the micro-plate reader was reduced to around one third of that with the ordinary UV-vis spectrophotometer. Therefore, the absorbance differences among the mutations (T2 - T5) will be lowered. In high-throughput analysis, we need to overcome the following defects: evaporation of the organic solvent during the measurements, resulting in gradually increasing the concentration of the sample DNA, and the mixing conditions of reverse micellar solutions in a 96-well plate format. The former may increase the degree of a duplex, but influence the reproducibility of the analysis. With respect to the latter, insufficient mixing in a 96-well plate may also be reflected to the extended time that was required to reach the equilibrium (note that the x-axis of Fig. 3A starts from after 10-min equilibration). However, these defects mainly rely on the setting of the apparatus, and can be technically overcome.

In conclusion, an accurate detection of a YMDD mutant of HBV has been demonstrated using a unique system consisting of reverse micelles. In addition to the original procedure using a UV-vis spectrophotometer, a 96-well micro-plate format could be applied to at least distinguish a normal gene from a mutated one. Since the technique is rather simple, the reverse-micellar assay system is applicable for a high-throughput SNPs detection with a non-labeled intact DNA sample.

References

1. S. D. Pas, R. A. de Man, E. Fries, A. D. M. E. Osterhaus, and H. G. M. Niesters, *J. Clin. Virol.*, **2002**, *25*, 63.
2. F. Suzuki, Y. Suzuki, A. Tsubota, N. Akuta, T. Someya, M. Kobayashi, S. Saitoh, Y. Arase, K. Ikeda, and H. Kumada, *J. Hepatol.*, **2002**, *37*, 824.
3. T. Kirishima, T. Okanoue, Y. Daimon, Y. Itoh, H. Nakamura, A. Morita, T. Toyama, and M. Minami, *J. Hepatol.*, **2002**, *37*, 259.
4. L. C. Park, T. Maruyama, and M. Goto, *Analyst*, **2003**, *128*, 161.
5. T. Maruyama, L. C. Park, T. Shinohara, and M. Goto, *Biomacromolecules*, **2004**, *5*, 49.
6. H. T. Allawi and J. Santalucia, *Nucleic Acid Res.*, **1998**, *26*, 2694.

Purification and Characterization of the Human Erythrocyte Band 3 Protein C-Terminal Domain†

Guohui Fu,*,‡ Tianying Wang,‡ Baofeng Yang,§ Fengxiang Lv,‡ Congning Shi,‡ Xiaoshu Jiang,‡ Lifeng Tian,‡ Weihan Yu,|| and Naotaka Hamasaki⊥

Departments of Pathophysiology and Pharmacology and The Institute for Keshan Disease, Harbin Medical University, Harbin 150086, China, and Department of Clinical Chemistry and Laboratory Medicine, Faculty of Medicine, Kyushu University, Fukuoka 812-8582, Japan

Received July 19, 2003; Revised Manuscript Received December 12, 2003

ABSTRACT: To clarify the function of the hydrophilic carboxyl-terminal tail of human erythrocyte membrane band 3 protein (HEM-B3), we purified two peptides, C1 (Ala893−Val911) and KS4 (Gly647−Arg656), from human erythrocyte band 3 protein preparations. Purified C1 peptides at concentrations from 5 to 80 μM were incubated with fresh human erythrocyte white ghosts. The C1 peptide demonstrated a novel protease activity, which cleaved glycophorin A (GPA) at Leu118−Ser119 in a dose-dependent manner. This activity was eliminated by trypsin. In a control experiment, the KS4 peptide did not cleave GPA under the same conditions. To help substantiate that the band 3 C-terminal tail peptide (C1) alone possesses the protease activity, two experiments were performed. First, the plasmids pGBKT$_7$-GPA-Ct and pGADT$_7$-AE1-Ct were cotransformed into the yeast strain AH109. The pGBKT$_7$-GPA-Ct plasmid contains the cDNA of the 33 amino acid residue section of GPA (Tyr93−Asn125) fused with the pGBKT$_7$ vector. The plasmid pGADT$_7$-AE1-Ct contains the cDNA of the C-terminal 33 amino acid residues of HEM-B3 fused with the GAL4 DNA-binding domain in the pGADT$_7$ vector. The results of the cotransformation experiment indicated that the C-terminal 33 amino acid residues of HEM-B3 interacted directly with the GPA C-terminal segment defined above. Second, we used a mammalian two-hybrid analysis to confirm the interaction relationship between the band 3 C-terminal segment and the GPA C-terminus. The C-terminus of GPA and the C-terminal 33 amino acid residues of HEM-B3 were subcloned into the DNA-binding domain and transcription activation domain vectors of the two-hybrid system, respectively. They were then cotransfected along with a chloramphenicol acetyltransferse (CAT) reporter vector into HeLa cells. The CAT activity measured in this experiment also indicated that there was interaction between the C-terminal 33 amino acid residues of HEM-B3 and the C-terminus of GPA.

Human erythrocyte membrane band 3 (HEM-B3;[1] anion exchanger 1, AE1) is a major integral membrane anion-exchange glycoprotein. It has a molecular mass of 95 kDa and composes about 25 wt % of the total membrane protein of the erythrocyte (*1*−*3*). HEM-B3 consists of three separate domains: the N-terminal (~403 residues) 43 kDa cytoplasmic domain, the C-terminal membrane-spanning domain, and the cytoplasmic carboxyl-terminal tail domain (*4*−*6*). The N-terminal 43 kDa domain, which is water soluble, anchors to the erythrocyte skeleton by association with ankyrin and protein 4.1. It also binds an array of other proteins including protein 4.2. It binds the glycolytic enzymes glyceraldehyde-3-phosphate dehydrogenase, alderase, and phosphofructokinase as well as tyrosine kinase p72^{syk} and deoxyhemoglobin (*7*).

The C-terminal membrane-spanning domain, which transverses the cell membrane 14 times, is a highly conserved domain. It catalyzes Cl^-/HCO_3^- anion transport across the phospholipid bilayer (*8*). It also serves as the major antigen responsible for immune-mediated removal of senescent and abnormal erythrocytes (*9*). The topology of this domain has been reported, and the amino acid residues important for anion transport have been identified (*10*). There is, however, little detailed information of the acidic carboxyl-terminal tail of HEM-B3 (from Asn880 to Val911). This portion of the HEM-B3 molecule contains many acidic amino acids and thus has a net negative charge. It has been shown to be inaccessible to trypsin even though it is highly hydrophilic (*11*), indicating that the binding sites must be hidden, perhaps by interaction with other proteins.

Over the past few years, several studies have been focused on the acidic C-terminal tail of the band 3 protein. It contains a binding site for carbonic anhydrase (CA) at Asp887−

† This work was supported in part by a grant from the Key Subject of the National Natural Science Foundation of China.

* Corresponding author. Tel: 86-0451-86666149. E-mail: figuhu@263.net.
‡ Department of Pathophysiology, Harbin Medical University.
§ Department of Pharmacology, Harbin Medical University.
|| The Institute for Keshan Disease, Harbin Medical University.
⊥ Department of Clinical Chemistry and Laboratory Medicine, Kyushu University.

[1] Abbreviations: ABTS, 2,2′-azinodi(3-ethylbenzothiazolinesulfonate) diammonium salt crystals; AE1, anion exchanger I; Ala, alanine; Arg, arginine; Asn, asparagine; Asp, aspartic acid; C1, Ala893−Val911 of band 3; CA, carbonic anhydrase; CAT, chloramphenicol acetyltransferse; ELISA, enzyme-linked immunosorbent assay; FRAP, fluorescence recovery after photobleaching; Gly, glycine; GPA, glycophorin A; HEM-B3, human erythrocyte membrane band 3 protein; KS4, Gly647−Arg656 of band 3; Leu, leucine; PBS, phosphate-buffered saline; PMSF, phenylmethanesulfonyl fluoride; Ser, serine; Tyr, tyrosine; Val, valine.

10.1021/bi035281c CCC: $27.50 © 2004 American Chemical Society
Published on Web 01/24/2004

Asp890, and the CA activity is required for full anion transport activity of the band 3 protein (*12*, *13*). Although deletion of the 11 C-terminal amino acids does not affect the overall structure or anion transport activity of the band 3 protein, it does affect the surface membrane trafficking of the protein (*14*, *15*). In the present paper, we purified and collected the two HEM-B3 peptides (C1 peptide, Ala893−Val911, and KS4, Gly647−Arg656) from human erythrocyte membranes and incubated them with fresh human erythrocyte white ghosts to investigate the function of the C1 peptide and to search for a protein, which may interact with the hydrophilic carboxyl-terminal tail of HEM-B3. In our experiments we found that the band 3 C1 peptide demonstrated a novel protease activity. It was found to cleave GPA, another transmembrane protein of the human erythrocyte, at the Leu118−Ser119 bond. The two-hybrid analysis showed that there is a direct interaction between band 3 Asn880−Val911 and GPA Tyr93−Asn125.

EXPERIMENTAL PROCEDURES

Preparation of Human Erythrocyte White Ghosts. Human erythrocyte white ghosts were prepared as previously described by Dongkang et al. (*11*). Briefly, human blood was washed four times in phosphate-buffered saline (PBS) to remove the white cells from the blood and then suspended in PBS containing 0.2 mg/mL trypsin at 37 °C for 1 h to digest glycophorins. The preparations were then washed with PBS containing PMSF (2.5 μg/mL) three times to remove the trypsin. The pellets were lysed by adding more than 20 volumes of 5 mM $NaHCO_3$ with stirring on ice for 5 min. The solution was centrifuged at 24000*g* for 30 min at 4 °C and washed with the same buffer four times at 4 °C. The packed ghosts were stored at −80 °C until they were used. White ghosts (1 mg/mL) in 5 mM $NaHCO_3$ containing 0.15 M NaCl were digested with 15 μg/mL trypsin at 4 °C for 1 h with stirring (i.e., trypsin treatment with high-salt concentration). The cytosolic 40 kDa domain of HEM-B3 was thereby cleaved. After addition of antipain (10 μg/mL), the treated membranes were separated by centrifugation at 45600*g* for 20 min at 4 °C and then washed extensively with more of the same buffer. Peripheral membrane proteins in the washed membranes were stripped with 5 volumes of 100 mM NaOH at 4 °C. The alkali-stripped membranes were washed with 5 mM $NaHCO_3$ three times and resuspended in 5 mM $NaHCO_3$ at a protein concentration of 1.5 mg/mL. The membrane suspension was redigested with 15 μg/mL trypsin at 37 °C overnight (i.e., trypsin treatment with low-salt concentration). The peptides released to the supernatant were collected by centrifugation at 27200*g* for 30 min at 4 °C.

Purification of C1 and KS4 Peptides. The C1 and KS4 peptides were obtained from the supernatant described above by using HPLC. The HPLC system was equipped with a reverse-phase column (Cosmosil C-18, 4.6 × 250 mm) using a gradient of acetonitrile containing 0.1% trifluoroacetic acid. It was run for 150 min at a flow rate 0.8 mL/min. An amino acid sequencer was used to determine the purity and concentration of the C1 and KS4 peptide-containing fractions.

Preparation of Fresh White Ghosts for Incubation Experiments. Human blood was washed with PBS four times, lysed in more than 20 volumes of 5 mM $NaHCO_3$, and stirred on ice for 5 min. The lysate was centrifuged at 24000*g* for 30 min at 4 °C. The pellets were washed twice with 5 mM $NaHCO_3$ and once with 5 mM $NaHCO_3$ containing 0.15 mM NaCl. The fresh white ghosts were diluted to 1 mg/mL for incubation experiments.

Incubation Experiments. The C1 peptides collected from the HPLC fraction were quantitated by the amino acid sequencer and then were added to experimental tubes at concentrations of 5, 10, 30, and 80 μM. The peptides were evaporated by speed vacuum, and then 300 μL of fresh white ghosts was added to the tubes. The samples were mixed well and incubated at 37 °C for 1 h. The incubated solution was centrifuged at 25000*g* for 30 min. The supernatant was removed for HPLC analysis.

Yeast Two-Hybrid Assay. A cDNA fragment encoding the C-terminal 33 amino acid residues of HEM-B3 was fused in frame with the GAL4 DNA-binding domain in the $pGADT_7$ vector to create the hybrid bait protein, while the 33 amino acid residues of glycophorin A were fused to the $pGBKT_7$ vector. Both of the reconstructed plasmids were introduced into a yeast reporter strain by the lithium acetate transformation procedure of Gietz et al. Transformants were allowed to grow at 30 °C for 2−4 days until colonies were large enough to assay for β-galactosidase activity. Transformant cells were then plated directly onto sterile Whatman no. 1 filters that had been layered onto sterile growth media. After colonies had grown, the filters were assayed for β-galactosidase activity. The cells were disrupted by a cycle of freezing the filter paper with the yeast colonies on it in liquid nitrogen and thawing to room temperature. Each filter was then soaked with 2 mL of Z buffer (CLONTECH Matchmaker protocol manual) containing 5-bromo-4-chloro-3-indolyl β-D-galactoside. The filters were then placed in a covered plastic container at room temperature and checked at 30 min intervals. The filters were then dried and photographed to record the data.

Mammalian Two-Hybrid Assay. The cDNA fragment of the AE1 C-terminus and the C-terminus of GPA were subcloned into the transcription activity domain vector pVP16 and DNA-binding domain pM, respectively. One day before transfection, HeLa cells were seeded at 5×10^5/plate in six 10 cm plates. Using the calcium phosphate transfection method, 2.0 μg of both the pM-based plasmid and pVP16-based plasmid, as well as 1.0 μg of reporter plasmid pG5CAT, was cotransfected into the HeLa cells. The detailed transfection protocol was provided with the kit purchased from CLONTECH. The cells were incubated at 37 °C in 3% CO_2 overnight and then carefully washed twice with 5 mL of PBS. Then 10 mL of complete medium with 10% fetal bovine serum was added. The cells were incubated for 24−48 h, harvested and lysed, and assayed for CAT activity using the CAT enzyme-linked immunosorbant assay kit (Roche Molecular Biochemicals). The cell extracts (containing CAT enzyme) were added to the wells of a microtiter plate that was precoated with a polyclonal antibody to CAT. All of the CAT in the cell extracts was bound to the CAT antibodies. Digoxigenin-labeled antibodies to CAT were then added to bind to CAT, and an antibody to digoxigenin conjugated to peroxidase was added to bind to the digoxigenin. Finally, the peroxidase substrate ABTS was added. The peroxidase enzyme catalyzed the cleavage of the substrate producing a color reaction. The absorbance of the

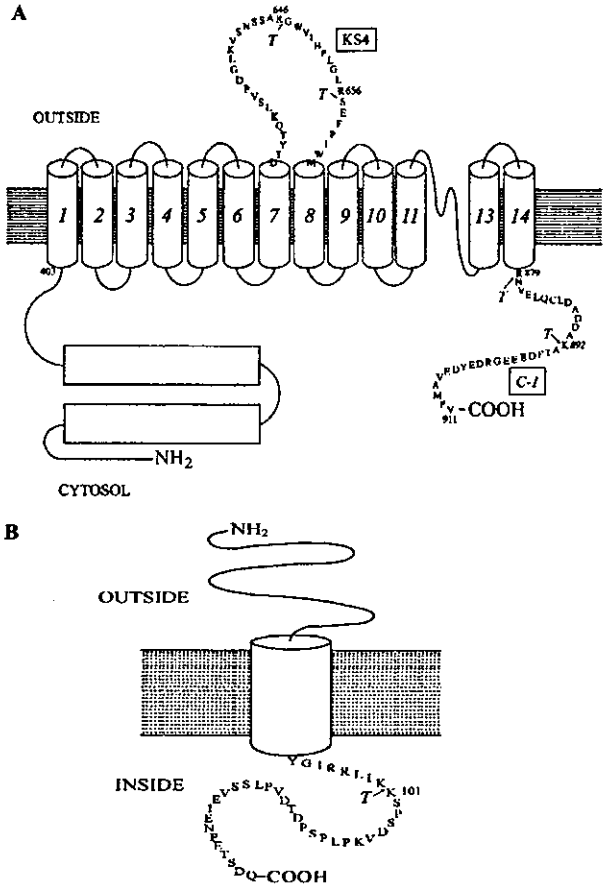

FIGURE 1: Topology model of band 3 and glycophorin A: (A) band 3; (B) glycophorin A.

sample was determined by an enzyme-linked immunosorbent assay reader and was directly correlated to the level of CAT present in the cell extracts.

RESULTS

Analysis of Peptides Released from the Erythrocyte Membrane. After removal of the cytosolic N-terminal domain of HEM-B3 and the peripheral membrane proteins, the transmembrane 55 kDa domain of HEM-B3 remained. The C1 and KS4 peptides were located at the intracellular and extracellular sides, respectively, of the erythrocyte membrane (Figure 1A, band 3; Figure 1B, GPA). The treated membranes were further digested with trypsin at 37 °C for 1 h, and the peptides released were analyzed by the standard HPLC procedure. Figure 2 shows the elution profile of one HPLC analysis. All major peaks were collected and rechromatographed with the same HPLC system. The purified peptides were sequenced by a gas-phase amino acid sequencer. The C1 and KS4 peptides were thus identified.

Analysis of Peptides Released from Fresh White Ghosts Which Were Incubated with C1 and KS4 Peptides. The purified C1 peptides were incubated with fresh white ghosts at 37 °C for 1 h at concentrations of 0−80 μM and then centrifuged at 15000*g*. The supernatant was analyzed by standard HPLC. Figure 3 shows the pattern obtained by HPLC analysis of the supernatant. The profile has a major peak at concentrations of 5 and 10 μM C1 peptide (panels A and B). We sequenced the fraction materials of the major peak. The sequencer data from the major peak fraction indicated the presence of the C1 peptide and the GPA Lys101−Asp130 sequence. However, when the C1 peptide concentration was increased up to 30 and 80 μM, the HPLC pattern produced by the supernatant changed from the one major peak produced at the lower concentrations to three peaks (panels C and D). The sequencer data identified the sequences of the material contained in each of the three peaks as follows: GPA Lys101−Leu118 (peak 1), GPA Ser119−Asp130 (peak 2), and C1 peptides (peak 3).

A Novel Protease Inactivated by Trypsin. To further investigate the properties of the C1 peptide of HEM-B3, six incubation experimental groups were performed. Group 1 had white ghosts only, group 2 had white ghosts + trypsin (15 μg/mL), group 3 had white ghosts + C1 peptides (40 μM), group 4 had white ghosts + C1 peptides + trypsin, group 5 had white ghosts + KS4 peptides (40 μM), and group 6 had white ghosts + KS4 peptides (40 μM) + trypsin. All of the incubated supernatants were analyzed by HPLC (Figure 4). In groups 1 and 2, no major peaks appeared in their HPLC profile (panels A and A′). Groups 5 and 6 showed one major peak that corresponded to the KS4 peptide sequence that was added to the incubation tube (panels C and C′). In group 3, the HPLC profile showed three major peaks: (peak 1) GPA Lys101−Leu118, (peak 2) GPA Ser119−Asp130, and (peak 3) C1, which are shown in panel B. However, in group 4, the three major peaks returned to a single peak (panel B′). The sequence data on this peak show the GPA Lys101−Asp130 and the C1 peptide sequence again. These results suggest that the preparation of purified C1 peptide has an unidentified protease activity, that it cleaves the amino acid bond of GPA at Leu118−Ser119, and that this protease activity was inactivated by trypsin. The amino acid sequencer profile indicates that the preparation contains no peaks corresponding to known protease sequences. Also, no peaks are seen which represent peptides as large as known proteases. In the control experiments using KS4, the peaks corresponding to GPA Lys101−Leu118 and GPA Ser119−Asp130 were not found, and no change occurred with the addition of trypsin to the incubation tubes. The presence of these results suggests that the HEM-B3 C-terminal tail might interact with the GPA C-terminal end and have a specific protease activity.

Yeast Two-Hybrid System Analysis of the AE1 C-Terminal End and C-Terminus of GPA. To test whether the AE1 C-terminal end Ala893−Val911 interacts with GPA Lys101−Asp130 directly, the cDNA coding for the entire 33 amino acid region of GPA was fused in frame to the GAL4 DNA-binding domain (in the vector pGBKT$_7$). Also, a cDNA coding for a 33 amino acid fragment of the AE1 C-terminus was fused to the GAL4 DNA-activating domain (in the vector pGADT$_7$). The two-hybrid plasmids were cointroduced into *Saccharomyces cerevisiae* AH109 cells, which contain the lacZ, his3, and ade reporter genes under different promoters with upstream GAL4 binding sites. Interaction of the two fusion proteins is necessary to juxtapose the GAL4 DNA-binding and activation domains, which then activate transcription of the reporter genes. We cultured the transformants on trp$^-$/leu$^-$/his$^-$/ade$^-$ medium in four separate groups, and then β-galactosidase activity was checked. Results of these experiments are shown in Table 1. Only the transformant, which was infected with pGBKT7-GPA-Ct and pGADT7-

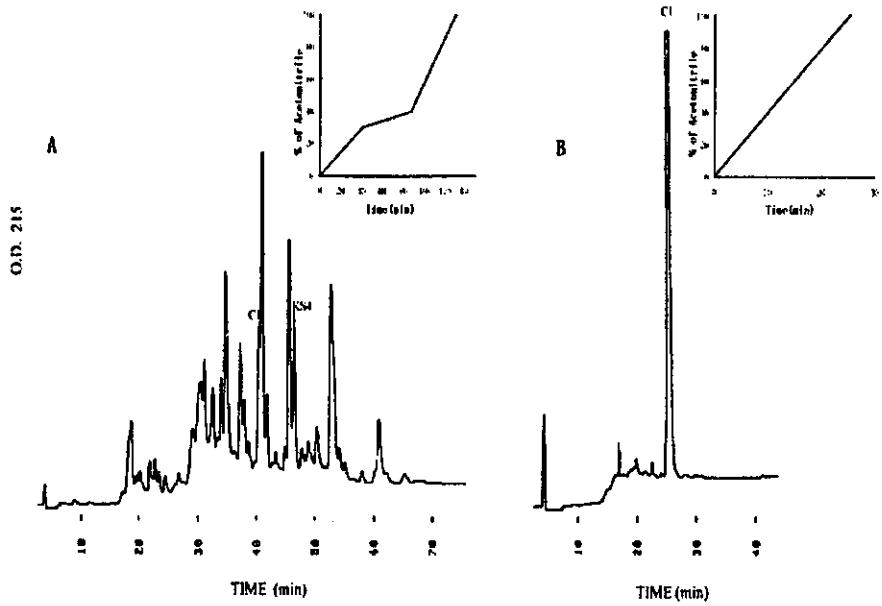

FIGURE 2: Purification of C1 and KS4 peptides from human erythrocyte membrane band 3 using reversed-phase Cosmosil C-18 columns. Panel A: Membranes were isolated from human erythrocytes, and the peripheral membrane proteins were removed with NaOH at 4 °C. After that, the cytosolic 40000 Da domain of band 3 was also removed by treating white ghosts with trypsin at 4 °C. Then the treated membranes were redigested with trypsin at 37 °C for 1 h. Peptides released into the supernatant were collected and analyzed using a gradient of acetonitrile containing 0.1% trifluoroacetic acid. Panel B: The collected C1 fraction was purified, and the single peak and amino acid sequencer data show the C1 peptide to be of high purity.

AE1-Ct, could grow on the $trp^-/leu^-/his^-/ade^-$ plate and possessed a β-galactosidase activity.

Mammalian Two-Hybrid Analysis. Figure 5 shows the interaction of the band 3 C-terminus and GPA C-terminus assessed by a mammalian two-hybrid system. HeLa cells were transfected with a DNA-binding-based vector, an activating-based vector, and a CAT reporter vector simultaneously. After treatment with lysozyme, cell extracts containing CAT were used immediately for CAT ELISA. The absorbance of the samples was measured at 405 nm using a microtiter plate reader. The absorbance of the cell extracts which were transfected with the pM-GPA-Ct and pVP16-AE1-Ct (group 1) was significantly higher than the negative control (groups 2, 3, 4, and 6). These results suggest that the C-terminus of band 3 interacts with the C-terminus of GPA.

DISCUSSION

Although the C-terminal 33 amino acid residue section of the band 3 protein contains two trypsin cleaving sites and is similar to the N-terminal domain in that it is very hydrophilic, the N-terminal cytoplasmic domain can be removed by treatment of the erythrocyte membrane with trypsin alone, whereas the C-terminal tail requires pretreatment with 100 mM NaOH to strip the erythrocyte membrane before trypsin will cleave it. This property led us to consider that the band 3 C-terminal 33 amino acid residues might interact with some other protein by ionic attraction. So, in the original experiment, we purified and collected band 3 C-terminal C1 peptides and incubated the C1 peptides with fresh white ghosts, expecting to draw off a protein from the erythrocyte membrane which would show a new band upon SDS−PAGE analysis of the supernatant. However, we were disappointed as no new interesting band was dyed when the incubated supernatant was run on SDS−PAGE (figure not shown). The supernatant was also analyzed by HPLC equipped with a reverse-phase column (Cosmosil, 4.6 × 250 mm). This method demonstrated that different major peptides were contained in the supernatant at different concentrations of C1 peptide. When the C1 peptide concentration reached 30 μM, the preparation of C1 peptide began to show a novel protease activity that cleaved the GPA C-terminus at Leu118−Ser119 and was inactivated by trypsin. The high purity of the C1 peptide preparation and the absence of peaks that represent peptides as large as known proteases in it indicate that the enzyme activity is closely related to the C1 peptide. The yeast two-hybrid and mammalian two-hybrid analyses showed that the C-terminal 33 amino acid residues of band 3 directly interact with the GPA C-terminus, supporting the idea that an enzyme−substrate relationship exists between them.

Several previous studies have suggested an interaction between HEM-B3 and GPA at an early stage in the biosynthesis and intracellular processing of the two proteins. It was initially observed that the glycosylation of HEM-B3 was altered in GPA-deficient En (a^-) red blood cells, as well as in other GPA mutant red blood cells (*16*, *17*). In addition, the fact that anti-GPA antibodies can reduce the rotational diffusion of HEM-B3 indicates that the two proteins may associate in the red blood cell membrane (*18*). This view is further strengthened by the observation that the binding of anti-GPA antibodies to its extracellular domain rigidifies the red blood cell membrane (*19*) and leads to the immobilization of both GPA and HEM-B3 as measured by the in situ FRAP (fluorescence recovery after photobleaching) technique (*20*). Furthermore, reconstitution of purified GPA and HEM-B3 in nonionic detergents indicates that GPA may directly associate with HEM-B3 (*21*). Immunological studies also

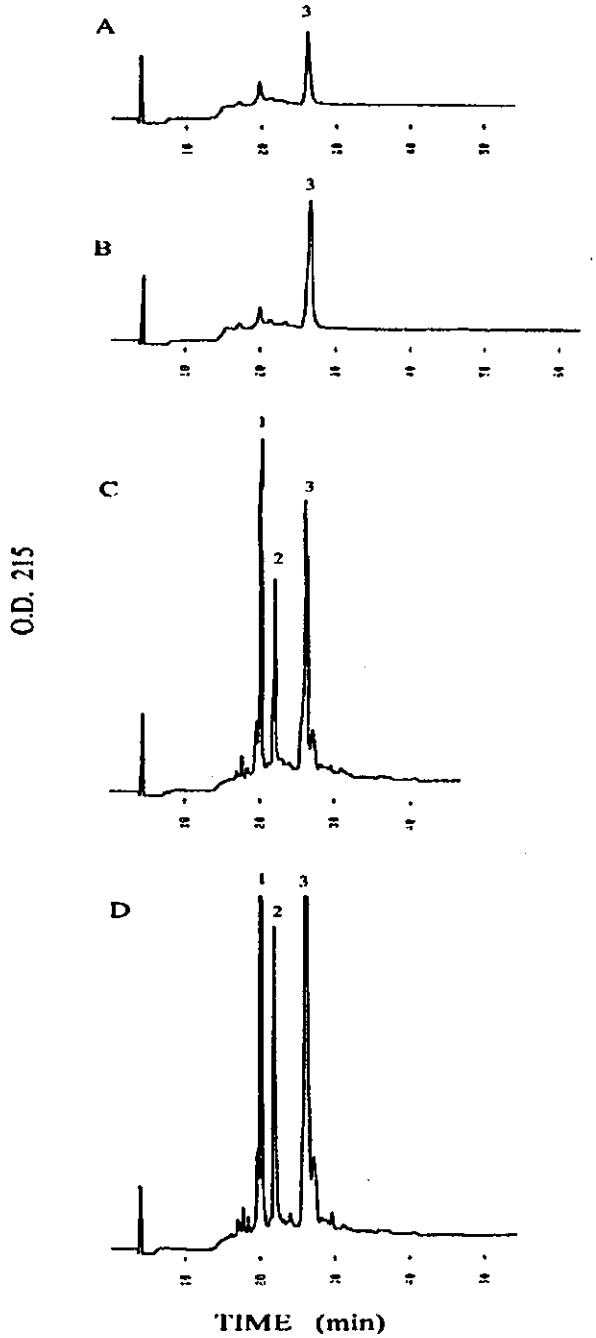

FIGURE 3: Effect of C1 peptide on fresh white ghosts. C1 peptides were purified from erythrocyte membranes, and 5, 10, 30, and 80 μM C1 peptide, respectively, was added to incubation tubes. After evaporation by speed vacuum, 1 mL of fresh white ghosts (1 mg/mL protein) was added to the tubes, and the mixture was incubated at 37 °C for 1 h. The supernatant was obtained by centrifugation at 15000g for 20 min. Analysis of peptides in the supernatant was carried out with a reversed-phase Cosmosil C-18 column. The major peaks were sequenced.

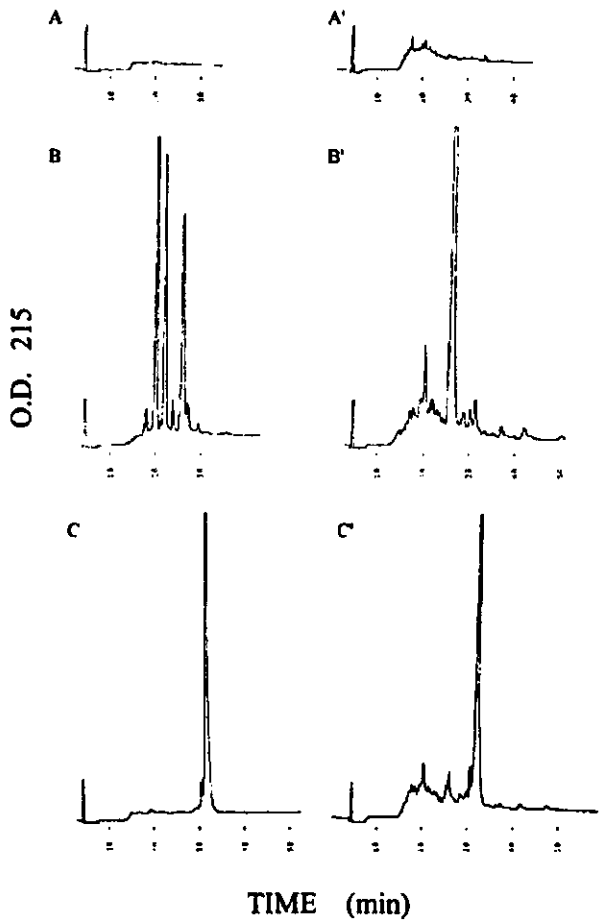

FIGURE 4: Specific analysis of C1 activity: (A) fresh white ghosts; (A') fresh white ghosts + trypsin; (B) fresh white ghosts + C1 peptides (40 μM); (B') fresh white ghosts + C1 peptides (40 μM) + trypsin (15 μg/mL); (C) white ghosts + KS4 peptides (40 μM) + trypsin (15 μg/mL); (C') white ghosts + KS4 peptides (40 μM) + trypsin (15 μg/mL).

Table 1: β-Galacosidase Activity Analysis[a]

DNA-binding domain	activating domain	β-galacosidase activity
$pGBKT_7$	$pGADT_7$	−
$PGBKT_7$-GPA-Ct	$pGADT_7$	−
$pGBKT_7$	$pGADT_7$-AE1-Ct	−
$PGBKT_7$-GPA-Ct	$pGADT_7$-AE1-Ct	+

[a] Yeast two-hybrid assay of the cytoplasmic C-terminus of band 3 and GPA. AH109 cells were cotransformed with pGADT7-AE1-Ct and pGBKT7-GPA-Ct, pGADT7 and pGBKT7, pGADT7 and pGBKT7-GPA-Ct, and pGADT7-AE1-Ct and pGBKT7, respectively, and then the β-galacosidase activity was measured. β-Galacosidase activity is shown as the average of five independent transformants ± SD. Only the transformants which cotransformed with the band 3 C-terminus and GPA C-terminus exhibited β-galacosidase activity.

support a close GPA−HEM-B3 interaction: a monoclonal antibody raised against HEM-B3 was shown to coprecipitate GPA from red blood cell membranes (*22*−*24*). Finally, the expression of the antithetical antigens Wr^a and Wr^b, which represent alternative polymorphisms of HEM-B3, requires an interaction between HEM-B3 and GPA involving a region of the transmembrane domain of GPA (*25*). The presence of additional blood group epitopes, which are dependent on the interaction of GPA with HEM-B3, was also suggested (*26*, *27*), and the existence of one such epitope was recently documented (*28*).

Recently, evidence is accumulating that GPA has a role in facilitating the movement of band 3 to the cell surface. Coexpression of wild-type band 3 cRNAs with GPA induces an increased level of band 3 mediated chloride influx in *Xenopus* oocytes by facilitating the translocation of band 3

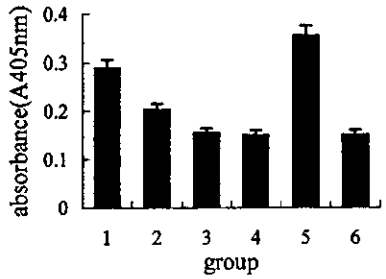

FIGURE 5: CAT activity values were measured by ELISA. The absorbance values are normalized by the CAT enzyme under standard dilutions, and the average value is calculated from three separate experiments (±SD). The absorbance of the experimental group increased remarkably when compared with the control groups ($p < 0.01$). Key: group 1, pM-GPA-Ct and pVP16-AE1-Ct; group 2, pM-GPA-Ct and pVP16; group 3, pM and pVP16-AE1-Ct; group 4, pM and pVP16; group 5, positive control pM3-VP; group 6, HeLa cells without transfection.

to the cell surface and potentially also by enhancing the anion transport function of HBM-B3 (*29*). Also, there is a close relationship between the hydrophilic carboxyl-terminal tail of band 3 and the cytoplasmic C-terminus of GPA. The cytoplasmic C-terminus of GPA is involved in the enhancement of band 3 protein movement to the cell surface. Deletion of the cytoplasmic C-terminus of GPA led to the loss of the ability to enhance band 3 specific chloride transport. The single point mutation GPA R97M (located on the cytoplasmic side of the transmembrane domain) also exhibited an impaired ability to increase the surface presentation of band 3 but efficiently enhances band 3 anion transport activity (*30*). These results imply that the cytoplasmic C-terminus of GPA is responsible for enhanced trafficking of the band 3 protein to the cell surface. The GPA-mediated enhancement of the band 3 surface presentation could be achieved either by direct interaction of the GPA C-terminus with band 3 or by interaction of the GPA C-terminus with other proteins which may facilitate band 3 trafficking. Taken together, these observations strongly suggest that GPA and HEM-B3 interact directly at the red blood cell membrane and that these interactions are associated with the movement of band 3 to the cell surface (*31*). Although recent studies have provided more clear information on the structure and function of HEM-B3 and its transmembrane and cytoplasmic domains, the direct interaction between GPA and band 3 has not yet been documented (*32*). In this paper, we focused on providing the evidence of the interaction between HEM-B3 Ala893−Val911 and GPA Tyr93−Asn125. Our experiments proved that the C-terminus of HEM-B3 interacts directly with GPA, and the interaction site was located in 32 amino acids of HEM-B3 and 33 amino acids of GPA.

The major new finding described here is that the segment of Asp893−Val911 of HEM-B3 interacts with GPA Lys101−Asn130 and is able to cleave it at the Leu118−Ser119 bond. At the present time, we do not know the natural tertiary structure that will demonstrate the enzyme activity. Also, the physiological meaning of the band 3 C-terminus protease activity and whether it has a function in any pathologic conditions are still uncertain. We believe that our work lays a good foundation for further studies of this peptide and provides clues for continuing research.

ACKNOWLEDGMENT

The authors thank Dr. Joseph R. Casey (Department of Physiology, University of Alberta, Alberta, Canada) for providing the band 3 gene. We also thank Drs. Zhiguo Wang (Department of Medicine, Montreal Heart Institute, Montreal, Canada) and Weidong Gao for reading the manuscript.

REFERENCES

1. Jay, D., and Cantley, L. (1986) *Annu. Rev. Biochem. 55*, 511−538.
2. Passow, H. (1986) *Rev. Physiol. Biochem. Pharmacol. 103*, 61−223.
3. Jennings, M. L. (1989) *Annu. Rev. Biophys. Biophys. Chem. 18*, 397−430.
4. Steck, T. L., Ramos, B., and Strapazon, E. (1976) *Biochemistry 5*, 1154−1161.
5. Zhu, Q., Lee, D. W. K., and Casey, J. R. (2003) *J. Biol. Chem. 278*, 3112−3120.
6. Low, P. S. (1986) *Biochim. Biophys. Acta 864*, 145−167.
7. Tanner, M. J. A. (2002) *Curr. Opin. Hemalol. 9*, 133−139.
8. Fujinag, J., Tang, X. B., and Casey, J. R. (1999) *J. Biol. Chem. 274*, 6626−6633.
9. Beckmann, R., Smythe, J. S., Jonathan, S., and Anstee, D. J. (1998) *Blood 92*, 4428−4438.
10. Kawano, Y., and Kenshi, O. (1988) *J. Biol. Chem. 263*, 8232−8238.
11. Dongchon, K., and Kenshi, O. (1992) *J. Biol. Chem. 267*, 19211−19217.
12. Sterling, D., Reithmeier, R. A. F., and Casey, J. R. (2001) *J. Biol. Chem. 276*, 47886−47894.
13. John, W. V., and Reithmeier, R. A. F. (2000) *Biochemistry 39*, 5527−5533.
14. Toye, A. M., and Lesley, J. (2002) *Blood 99*, 342−347.
15. Karet, F. E., and Gainza, F. J. (1998) *Proc. Natl. Acad. Sci. U.S.A. 95*, 6337−6342.
16. Gahmberg, C. G., Myllyla, G., Leikola, J., and Pirkola, A. (1976) *J. Biol. Chem. 251*, 6108−6116.
17. Sheetz, M. P., and Sawyer, D. (1978) *J. Supramol. Struct. 8*, 399−412.
18. Nigg, E. A., Bron, E. A., and Girardel, M. (1980) *Biochemistry 19*, 1887−1893.
19. Chasis, J. A., and Schrier, S. L. (1989) *Blood 74*, 2562−2568.
20. Chasis, J. A., Reid, M. E., and Jensen, R. H. (1988) *J. Cell Biol. 107*, 1351−1357.
21. Knowles, D. W., Chasis, J. A., and Evans, E. A. (1994) *Biophys. J. 66*, 1726−1732.
22. Dahr, W., Wilkinson, S., and Issitt, P. D. (1986) *Biol. Chem. Hoppe-Seyler 367*, 1033−1045.
23. Telent, M. J., and Chasis, J. A. (1990) *Blood 76*, 842−848.
24. Ring, S. M., Tippett, P., and Swallow, D. A. (1994) *Vox Sang. 67*, 226−230.
25. Wainwrite, S. D., Tanner, M. J. A., and Martin, G. E. M. (1989) *Biochem. J. 258*, 211−220.
26. Huang, C. H., Reid, M. E., and Xie, S. S. (1996) *Blood 87*, 3942−3947.
27. Leddy, J. P., Wilkinson, S. L., and Kissel, G. E. (1994) *Blood 84*, 650−656.
28. Bruce, L. J., Ring, S. M., and Anstee, D. J. (1995) *Blood 85*, 541−547.
29. Jarolim, P., Moulds, J. M., and Rubin, H. L. (1996) *Blood 88*, 4366−4374.
30. Groves, J. D., and Tanner, M. J. A. (1992) *J. Biol. Chem. 267*, 22163−22170.
31. Mark, T. Y., and Tanner, M. J. A. (2003) *J. Biol. Chem.* (in press).
32. Mark, T. Y., Beckmann, R., and Toye, A. M. (2000) *Biochem. J. 350*, 53−60.
33. Hassoun, H., Hanada, T., and Lutchman, M. (1998) *Blood 91*, 2146−2151.

BI035281C

Clin Chem Lab Med 2004;42(1):79–83 © 2004 by Walter de Gruyter • Berlin • New York

Analytical goals for coagulation tests based on biological variation

Yui Wada, Masako Kurihara, Mitsuko Toyofuku, Minako Kawamura, Hiroko Iida, Yuzou Kayamori, Sachiko Kinoshita and Naotaka Hamasaki*

Department of Clinical Chemistry and Laboratory Medicine, Kyushu University Hospital, Fukuoka, Japan

Abstract

Allowable imprecision and bias reference limits for laboratory data can be calculated based on measurements of biological variation. Although biological variation of clinical chemical data has been reported from many laboratories, there have been few reports of biological variation in coagulation tests. In this study, we calculated the biological variation of 13 coagulation tests in the clinical laboratory of Kyushu University Hospital and determined allowable imprecision and bias limits of variation. The participating subjects were 17 healthy individuals: three males and two females in their 20s, two males and two females in their 30s, one male and four females in their 40s, and two males and one female in their 50s. Monthly measurements were performed before breakfast 12 times from June 2001 to May 2002 and allowable imprecision and bias limits were calculated. Taken together with coefficient of variation of control plasma used in daily laboratory work at the hospital, the allowable imprecision limits of intra-laboratory variation determined in this study appear to be in attainable ranges.

Keywords: allowable bias; allowable imprecision; biological variation; inter-subject variation; intra-subject variation.

Introduction

In current laboratory practice, it is not rare for common reference intervals to be used among several laboratories or within a particular area. In order to share data and reference intervals among laboratories, variations in laboratory data must be maintained within allowable imprecision and bias limits. In 1970, Harris et al. (1) categorized variations of laboratory data into biological variations and analytical errors. Gowans et al. (2) proposed analytical goals for the acceptance of common reference intervals by laboratories throughout a geographical area, and biological variations of healthy individuals have been used for evaluating variations of laboratory data. Stöckl et al. (3) and Fraser et al. (4, 5) recommended methods for calculating allowable imprecision and bias. In clinical laboratory science, data on biological variations have mainly been applied to clinical chemical test items (6, 7). To our knowledge, however, there are few publications on intra-subject and inter-subject biological variation in prothrombin time (PT) and activated partial thromboplastin time (APTT) (8, 9).

Previously, we estimated allowable imprecision and bias limits using the biological variation of clinical chemical test items (10). In the present study, we further attempted to establish allowable imprecision and bias limits using biological variations of 13 coagulation tests.

*Corresponding author: Naotaka Hamasaki, MD, PhD, Department of Clinical Chemistry and Laboratory Medicine, Kyushu University Hospital, 3-1-1 Maidashi Higashi-ku Fukuoka 812-8582, Japan
Phone: +81-92-642-5748, Fax: +81-92-642-5770,
E-mail: hamasaki@cclm.med.kyushu-u.ac.jp

Materials and methods

Materials

The participating subjects were 17 members of our department: three males and two females in their 20s, two males and two females in their 30s, one male and four females in their 40s, and two males and one female in their 50s. Monthly blood samples were obtained before breakfast from June 2001 to May 2002. Each 4.5-ml blood sample was collected into a sampling tube containing 0.5 ml of 0.107 mol/l sodium citrate and centrifuged at 3000 rpm (1980 *g*) for 15 min and the plasma was used for the coagulation tests. "Standard plasma" for determination of the reference intervals in the 13 coagulation tests was obtained by collecting blood from healthy individuals (30 males and 30 females) before breakfast. Plasma from these 60 healthy subjects was pooled to yield "standard plasma", stored at −80°C, then thawed in a water bath at 37°C for 3 min and mixed by inversion immediately before use. Separately, we also prepared "normal pooled plasma" for daily monitoring use as "control plasma" for which values of the 13 coagulation tests were within the reference intervals.

Measurements

Items included in the coagulation tests were PT, APTT, fibrinogen (Fib), thrombotest (TB), antithrombin (AT), α_2-plasmin inhibitor (α2PI), plasminogen activity (PLG), thrombin-antithrombin complex (TAT), α_2-plasmin inhibitor-plasmin complex (PIC), thrombomodulin (TM), plasminogen activator-tissue plasminogen activator inhibitor-1 complex (tPAI-C), protein S (PS) and protein C (PC). Table 1 shows the analytical methods, representation methods, reagents, calibrators and measurement apparatuses used for these factors.

Table 1 Laboratory assays in coagulation tests.

Factors	Methods	Units	Kits manufacturers	Standards manufacturers	Automatic analyzers manufacturers
PT	Clotting time methods	seconds, %, INR	Thromborel^{R} S Dade Behrig, Germany	Standard plasma	MDA180 Haemostasis Bio Merieux, USA
APTT	Clotting time methods	seconds	MDA Platelin LS Bio Merieux, USA	Standard plasma	MDA180 Haemostasis Bio Merieux, USA
Fib	Clotting time methods	g/l	MDA Fibriquik Bio Merieux, USA	MDA verify reference plasma Bio Merieux, USA	MDA180 Haemostasis Bio Merieux, USA
TB	Clotting time methods	%	Thrombotest^{R} owren Axis-Shield Poc AS, Norway	Standard plasma	MDA180 Haemostasis Bio Merieux, USA
AT	Chromogenic substrate	%	MDA Antithrombin III Bio Merieux, USA	Standard plasma	MDA180 Haemostasis Bio Merieux, USA
α2PI	Chromogenic substrate	%	Testzym·neo APL Chromogenix, Sweden	MDA verify reference plasma Bio Merieux, USA	MDA180 Haemostasis Bio Merieux, USA
PLG	Chromogenic substrate	%	MDA Plasminogen Bio Merieux, USA	MDA verify reference plasma Bio Merieux, USA	MDA180 Haemostasis Bio Merieux, USA
TAT	EIA	ng/ml	TAT test·F Sysmex, Japan	TAT Standard Sysmex, Japan	Elsia F750 Sysmex, Japan
PIC	EIA	μg/l	PIC test·F Sysmex, Japan	PIC Standard Sysmex, Japan	Elsia F750 Sysmex, Japan
TM	EIA	TU/ml	TM test·F Sysmex, Japan	TM Standard Sysmex, Japan	Elsia F750 Sysmex, Japan
tPAI-C	EIA	ng/ml	tPAI-C test·F Sysmex, Japan	tPAI-C Standard Sysmex, Japan	Elsia F750 Sysmex, Japan
PS	Clotting time methods	%	Staclot Protein S Diagnostica Stago, France	Standard plasma	MDA180 Haemostasis Bio Merieux, USA
PC	Clotting time methods	%	Staclot Protein C Diagnostica Stago, France	Standard plasma	MDA180 Haemostasis Bio Merieux, USA

Calculation methods

Data from laboratory assays of coagulation are affected by liver dysfunction and inflammatory reactions because coagulation factors are produced in the liver and inflammatory reactions interfere with coagulation tests. To eliminate these effects, coagulation tests were performed with simultaneous measurements of white blood cell (WBC), aspartate aminotransferase (AST), alanine aminotransferase (ALT) and C-reactive protein (CRP). Reference intervals of WBC, AST, ALT and CRP were set as $3.50–9.00\times10^3/\mu l$, ≤ 33 U/l, ≤ 42 U/l in males and ≤ 27 U/l in females, and ≤ 2 mg/l, respectively. Intra-subject variation (CV_I) and inter-subject variation (CV_G) were calculated after exclusion of subjects whose data deviated from these reference intervals.

Through a one-way analysis of variance we calculated intra-subject variance (SI^2) and inter-subject variance (SG^2), and also determined analytical variance (SA^2) using the long-term variance of the "control plasma" (normal pooled plasma). Intra-subject variance (SI^2) and inter-subject variance (SG^2) were significantly different. Therefore, using these parameters, intra-subject variation (CV_I) and inter-subject variation (CV_G) were calculated as $CV_I=[SI^2-SA^2]^{1/2}/\text{mean}\times100$ and $CV_G=[(SG^2-SI^2)/12]^{1/2}/\text{mean}\times100$, respectively (1, 11). The allowable imprecision and bias limits for intra-laboratory variation (CV_A) and inter-laboratory variation (B_A) were calculated as desirable performance $CV_A<0.5\ CV_I$ and $B_A<0.25[CV_I^2+CV_G^2]^{1/2}$, as minimum performance $CV_A<0.75\ CV_I$ and $B_A<0.375[CV_I^2+CV_G^2]^{1/2}$, respectively (3–5).

Validation of intra-laboratory allowable imprecision limits (CV_A)

The values of CV_A were compared with the latest coefficient of variation (CV%) of the "control plasma" (normal pooled plasma) used for daily analyses.

Results

Biological variation and allowable imprecision and bias limits for laboratory coagulation tests

As described in Materials and Methods, blood specimens from 17 subjects were collected monthly from June 2001 to May 2002 (total number of measurements=204) and the coagulation test items listed in Table 1 were measured for all of these specimens. To eliminate the effects of inflammation and liver dysfunction, coagulation tests were performed with simultaneous measurements of WBC, AST, ALT and CRP. Intra-subject variation (CV_I) and inter-subject variation (CV_G) were calculated after exclusion of subjects whose data deviated from the reference intervals (after exclusion, the total number of measurements used for calculation was 170). Table 2 shows CV_I, CV_G, CV_A and B_A for the coagulation test data.

Verification of allowable imprecision limits for intra-laboratory variation (CV_A)

The CV_A calculated from the data for each test item was compared with the coefficient of variation (CV%) of the "control plasma" (normal pooled plasma) used for daily analyses. In Table 2, the CV% items marked with asterisks (*) were within the CV_A of the coagulation test items. Eleven items of the coagulation tests fell within the CV_A, but four items did not (Table 2).

Discussion

We have determined allowable imprecision and bias limits based on biological variation for 13 coagulation tests in 17 healthy individuals. Data from these coagulation tests can vary depending on the condition of subjects at the time of blood sampling; for example, the presence or absence of inflammation or liver dysfunction. To exclude values that deviated from reference intervals because of such factors, we excluded subjects with abnormalities of liver function according to measurements of AST and ALT, and those with inflammation according to measurements of WBC and CRP.

Although the number of subjects in this study was relatively low, we carefully eliminated the effects of inflammation and liver dysfunction so that our coagulation test data purely reflected the variations of coagulation function within individuals. In Table 2, we compared our CV_Is with previously published results (8, 9, 12). All CV_Is reported in 1985 by Costongs et al. (8) were larger than those in the present study. This difference may be due to improved analytical methods since 1985 and to the inclusion of smokers (n=126) and women taking oral contraceptives (n=61) among the large number of subjects (n=274) examined by Costongs et al. (8). All of the subjects in the present study were non-smokers and none of the women were taking oral contraceptives. CV_Is reported in 1992 by Dot et al. (9) were relatively consistent with our results (Table 2). Chambless et al. (12) reported short-term (1–2 week) CV_Is of APTT, Fib, and AT, all of which were about half of those reported in our present study (Table 2), suggesting that short-term CV_I is smaller than long-term (1 year) CV_I.

In the present study, we examined biological variations not only of PT, APTT, Fib, AT, α2PI and PLG, but also of TB, TAT, PIC, TM, tPAI-C, PS and PC, which have not been previously examined (Table 2). It is quite valuable to determine the biological variations and the allowable imprecision and bias of these coagulation tests, as these laboratory tests are important in screening for thrombophilia (13). PT and APTT are the most prevalent coagulation tests, which have been measured by a wide variety of combinations of reagents derived from different organs, principles of measurements used in the measuring apparatuses, and standard plasma selected. According to the PT-INR survey data of the Kyushu geographical area in 2001, the coefficient of variation in specimens from healthy individuals was 4.5% in all laboratories (n=133), 3.7% with reagent A (n=51), 3.9% with reagent B (n=27) and 4.8% with reagent C (n=38) (data not shown). These coefficients of variation were larger than the values of B_A% (1.3%, 1.9%) calculated in the present study (Table 2). However, as the intra-laboratory variation (CV_A) was small (Table 2), inter-lab-

Table 2 Coagulation tests: biological variation and the allowable imprecision and bias limits for laboratories.

Coagulation tests	Units	Mean	Biological variation		Imprecision	Bias	"Control plasma"		Other reports		
			Intra-subject CV_I, %	Inter-subject CV_G, %	Intra-laboratory CV_A, %	Inter-laboratory B_A (*2 B_A), %	2002 (1/11-30/11, n: 20)		1985 Ref. 8*3	1992 Ref. 9*4	1992 Ref. 12*5
							Mean	CV, %	CV_I, %	CV_I, %	CV_I, %
PT	seconds	11.3	2.4	4.0	1.2	1.2 (1.7)	11.4*1	1.0			
	%	99.2	5.6	9.4	2.8	2.7 (4.1)	95*1	2.4			
	INR	1.01	3.0	4.0	1.4	1.3 (1.9)	1*1	1.2	5.8	2.3	
APTT	seconds	29	3.3	7.1	1.6	2.0 (3.0)	27.7*1	0.6	6.8	2.1	1.7
Fib	g/l	2.3	8.7	14.8	4.4	4.3 (6.5)	3.4*1	2.1	10		6.8
TB	%	78.4	12.9	12.9	6.5	4.6 (6.8)	73*1	1.9			
AT	%	105.5	2.1	2.6	1.1	0.8 (1.2)	98	2.3	3.1		1.1
α2PI	%	115.7	4.8	7.1	2.4	2.1 (3.2)	105	4.4	5.8		
PLG	%	111.1	4.2	10.5	2.1	2.8 (4.2)	114	3.0	7.7		
TAT	ng/ml	1.0	26.0	20.0	12.9	8.1 (12.1)	4.4*1	2.8			
PIC	μg/ml	0.5	18.0	26.0	8.4	7.3 (11.0)	1.3*1	3.0			
TM	TU/ml	8.8	11.4	16.5	5.7	5.0 (7.5)	14.5*1	1.7			
tPAI-C	ng/ml	8.3	15.9	31.2	7.9	8.7 (13.1)	11.5*1	3.6			
PS activity	%	103.5	7.6	22.3	3.8	5.9 (8.8)	91	5.9			
PC activity	%	101.5	7.9	17.5	4.0	4.8 (7.2)	91*1	3.1			2.1 (antigen)
Number of subjects			17						274	39	39
Intervals			Monthly						Monthly	Monthly	1-2 weeks
Terms or times			Twelve months						Six months	Nine months	Three times

*1:Control plasma CV% < intra-laboratory CV_A%; *2B_A:Minimum performance for allowable bias; *3:Reference 8 (Netherlands), *4: Reference 9 (Spain), *5: Reference 12 (North Carolina).

oratory variation is expected to approach the value calculated in this study as the standardization of coagulation tests progresses.

Recently, the European Concerted Action on Thrombosis (ECAT) monitored plasma AT activity using data from 82 laboratories from 1996 to 1999 (14). On the basis of the reported CV_Is (8, 12), none of the laboratories in the ECAT study fulfilled the criterion of $CV_A < 0.5\ CV_I$; if the total biological variation for AT was calculated as 10.5% on the basis of the CV_I and CV_G data reported by Chambless et al. (12), 20% of the participating laboratories fulfilled the goal for diagnostic testing. This indicates that, at the present time, only a limited number of laboratories can overcome the allowable imprecision on the basis of biological variation of long-term analytical performance of coagulation tests.

In this study, we determined the allowable imprecision (CV_A) and bias (B_A) limits of 13 coagulation tests. The determined CV_A of the 15 items in the 13 coagulation tests are considered to be sufficiently attainable when compared with the coefficient of variation of the "control plasma" (normal pooled plasma) but it would not be easy to apply the CV_A to the intra-laboratory variation used in external quality assessment.

Acknowledgements

This work was supported in part by a Grant-in-Aid for Scientific Research from the Medical Promotion Foundation to SK and by the Ministry of Education, Science, Sports and Culture of Japan to NH.

References

1. Harris EK, Kanofsky P, Shakarji G, Cotlove E. Biological and analytical components of variation in long-term studies of serum constituents in normal subjects. Clin Chem 1970;16:1022–7.
2. Gowans EMS, Petersen PH, Blaabjerg O, Hørder M. Analytical goals for the acceptance of common reference intervals for laboratories throughout a geographical area. Scand J Clin Lab Invest 1988;48:757–4.
3. Stöckl D, Baadenhuijsen H, Fraser CG, Libeer JC, Petersen PH, Ricos C. Desirable routine analytical goals for quantities assayed in serum. Discussion paper from the members of the External Quality Assessment (EQA) working group A on analytical goals in laboratory medicine. Eur J Clin Chem Clin Biochem 1995;33:157–69.
4. Fraser CG, Petersen PH, Libeer JC, Ricos C. Proposals for setting generally applicable quality goals solely based on biology. Ann Clin Biochem 1997;34:8–12.
5. Fraser CG, Petersen PH. Analytical performance characteristics should be judged against objective quality specifications [editorial]. Clin Chem 1999;45:321–3.
6. Sebastian-Gambaro MA, Liron-Hemandez FJ, Fuentes-Arderiu X. Intra- and inter-individual biological variability data bank. Eur J Clin Chem Clin Biochem 1997;35:845–52.
7. Fuentes-Arderiu X. Variability of the biological variation. Scand J Clin Lab Invest 2002;62:561–4.
8. Costongs GMPJ, Bas BM, Janson PCW. Short-term and long-term intra-individual variations and critical differences of coagulation parameters. J Clin Chem Clin Biochem 1985;23:405–10.
9. Dot D, Miro J, Fuentes-Arderiu X. Within-subject and between-subject biological variation of prothrombin time and activated partial thromboplastin time. Ann Clin Biochem 1992;29:422–5.
10. Kinoshita S, Toyofuku M, Iida H, Wakiyama M, Kurihara M, Nakahara M, et al. Standardization of laboratory data and establishment of reference intervals in the Fukuoka prefecture: a Japanese perspective. Clin Chem Lab Med 2001;39:256–62.
11. Hosogaya S, Kume S. Biological variation and allowable error limits of the laboratory data. Jpn Lab Tech 1996;24:993–9.
12. Chambless LE, McMahon R, Wu K. Short-term intra-individual variability in hemostasis factors: the ARIC study. Atherosclerosis Risk in Communities Intraindividual Variability Study. Ann Epidemiol 1992;2:723–33.
13. Tsuda H, Hattori S, Tanabe S, Iida H, Nakahara M, Nishioka S, et al. Screening for aetiology of thrombophilia: a high prevalence of protein S abnormality. Ann Clin Biochem 1999;36:423–32.
14. Meijer P, de Maat MPM, Kluft C, Haverkate F, van Houwelingen HC. Long-term analytical performance of hemostasis field methods as assessed by evaluation of the results of an external quality assessment program for antithrombin. Clin Chem 2002;48:1011–5.

Received May 5, 2003, accepted July 31, 2003

Letter to the Editor

Development of a new colorimetric method for protein S activity measurement

Tomohide Tsuda[1,2,*], Hajime Yoshimura[1] and Naotaka Hamasaki[2]

[1] Shinotest Corporation, Kanagawa, Japan
[2] Department of Clinical Chemistry and Laboratory Medicine, Kyushu University Hospital, Fukuoka, Japan

Keywords: assay method; coagulation factor; colorimetric method; measurement; protein S; protein S activity; reconstruction; S-2238.

Development of a reliable method (simple, sensitive and accurate) for protein S measurement is needed (1–4), as the protein C/protein S coagulation regulatory system has been shown to be involved in thrombosis (5–16). This letter describes a new colorimetric method we have recently developed for measuring protein S activity. This method, unlike conventional ones that measure clotting time, measures protein S activity colorimetrically using chromogenic substrates. The principle of this assay system is that protein S activity is calculated by analyzing the correlation between protein S activity and thrombin production rate in the protein C/protein S coagulation regulatory system and the blood clot reaction system reconstructed in vitro (17, 18). Using this method, protein S activity was measured in a variety of samples and their values were compared to those obtained with the conventional method measuring clotting time (19).

Human activated protein C (APC), human protein S and human prothrombin, used in the assay, were obtained from Enzyme Research Laboratories, Inc. (South Bend, SD, USA), purified bovine factor Xa (FXa) from New England Biolabs, Inc. (Beverly, MA, USA), purified human factor Va (FVa) from Hematologic Technologies, Inc. (Essex Junction, VT, USA), thrombin chromogenic substrate S-2238 (20) from Chromogenix-Instrumentation Laboratory (Milan, Italy), bovine serum albumin (BSA) from Sigma-Aldrich Co. Ltd. (St. Louis, MS, USA) and porcine liver L-α-phosphatidylethanolamine (PE), porcine liver L-α-phosphatidylcholine (PC) and bovine brain L-α-phosphatidylserine (PS) from DOOSAN Serdary Research Laboratories (Yongin, Korea). A clot-time assay kit, STA®-Staclot® Protein S (Diagnostica Stago, Asnières, France), was used for comparison with our new method. A calibrator was made with purified protein S added to protein S-deficient plasma, and the activity was expressed as μg/ml PS-equivalent. Protein S-deficient plasma was prepared from fresh plasma by immunoadsorption on an anti-protein S immnoglobulin G (IgG) monoclonal antibody (3) column. Phospholipid (PE/PC/PS = 50/20/30 moles) and phospholipid (PC/PS = 80/2 moles), at the specified compositions, were taken into a test tube and, following evaporation of CHC_3 with N_2 gas, were re-suspended in distilled water and sonicated at 60°C for 10 minutes.

Protein S activity was measured as follows. Samples (4 μl) were incubated at 37° C for 10 minutes in a total volume of 100 μl containing 344 pmol/l APC and 10 μmol/l phospholipid PC/PS in buffer A (50 mmol/l Tris-HCl, pH 7.5, 0.15 mol/l NaCl, and 0.1% BSA). After addition of 100 μl containing 331 pmol/l FVa, 10 μmol/l phospholipid PC/PS and 5 mmol/l CaC_2 in buffer A, the mixture was further incubated for 10 minutes at 37° C (to degrade FVa by APC and protein S). During this incubation, 88 pmol/l FXa, 15 μmol/l phospholipid PE/PC/PS and 10 mmol/l $CaCl_2$ in 180 μl buffer A were mixed in a cuvette with 1.4 μmol/l prothrombin and 1.5 mmol/l S-2238 in 180 μl buffer A. Into this cuvette, the reaction mixture (180 μl), after incubation, was added and incubated at 37° C for measurement of non-degraded FVa activity. The absorbance at 405 nm was recorded for 40 minutes.

The principle of this method is shown schematically in Figure 1A. First, APC, protein S and FVa are incubated to hydrolyze FVa by APC and protein S (reaction 1). Since APC activity is increased by protein S, protein S activity can be measured from unhydrolyzed FVa. The remaining FVa activity is measured from the rate of thrombin production using the FXa and prothrombin reactions. Thrombin activity is obtained by measuring p-nitroaniline released from S-2238 as the absorbance at 405 nm (reaction 2). Figure 1B shows the time course of the reaction measured by the method described above. Since remaining FVa activity and protein S activity show an inverse relationship, the absorbance decreases as protein S activity increases.

Since thrombin is produced at a constant rate in this system, p-nitroaniline production increases at a constantly increasing rate. Therefore, the absorbance increases in proportion to the square of the reaction

*Corresponding author: Tomohide Tsuda, Shinotest Corporation, 2-29-14 Oonodai Sagamihara, Kanagawa, 229-0011, Japan
Phone: +81-42-753-0354, Fax: +81-42-786-8553,
E-mail: tomohide.tsuda@shino-test.co.jp

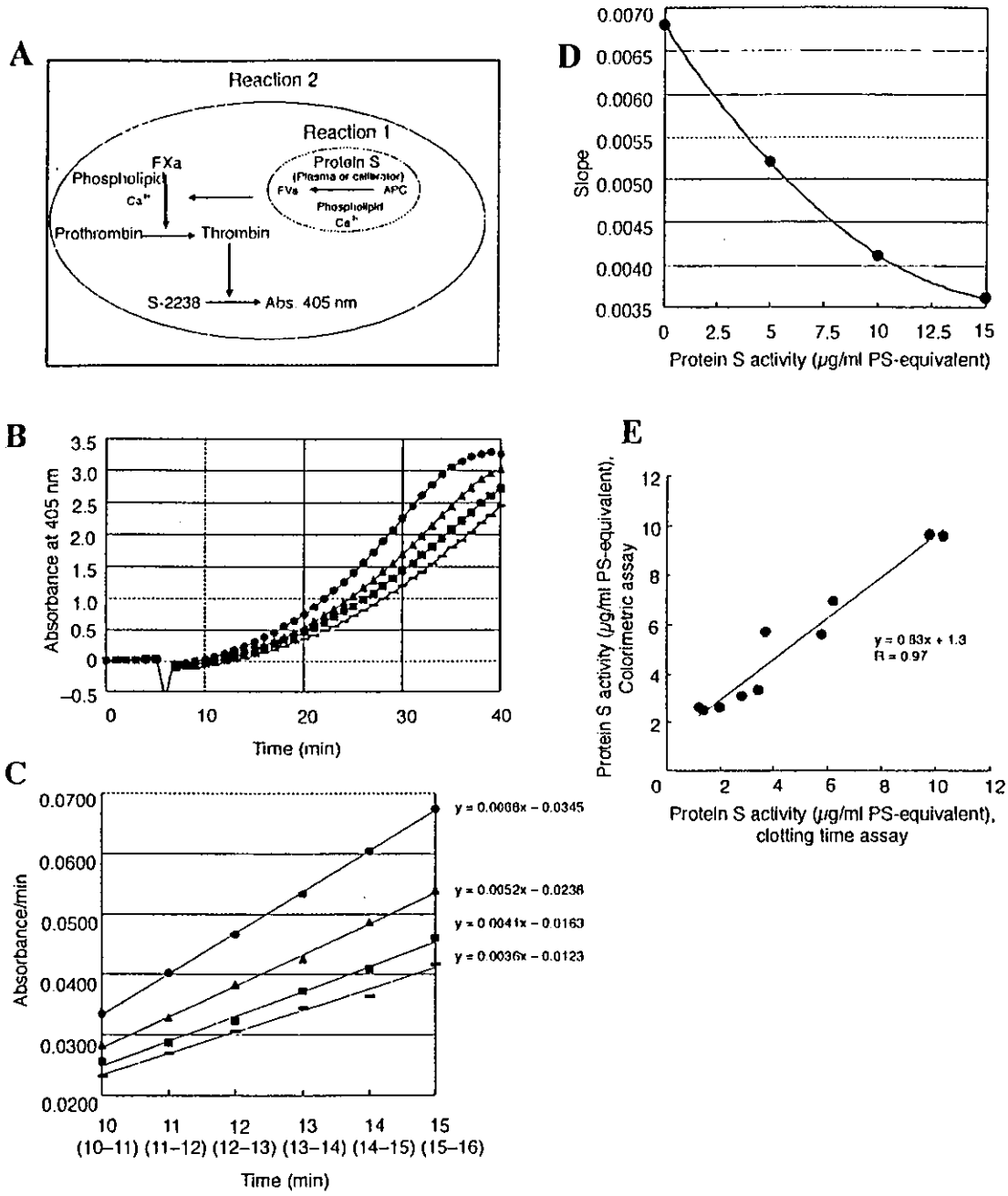

Figure 1 Method for protein S activity measurement using chromogenic substrates. A: Schematic diagram of protein S activity assay system. FVa degradation is produced by the reaction of APC, protein S and FVa (reaction 1). The reaction mixture is then added to a mixture of FXa, prothrombin and S-2238 to induce the enzymatic reaction cascade. Thrombin, thus generated, catalyzes the release from S-2238 of p-nitroaniline, which is measured as absorbance at a wavelength of 405 nm (reaction 2). The rate of p-nitroaniline generation depends on remaining FVa activity, which depends on protein S activity. B: Time course of thrombin production measured by the protein S assay system for constructing a protein S calibrator. FXa, prothrombin and S-2238 in 360 μl were pre-incubated for 5 minutes and then added to 180 μl reaction mixture containing APC, protein S and FVa. Absorbance was recorded for 40 minutes. Protein S activity was as follows: 0 (●), 5 (▲), 10 (■) and 15 μg/ml PS-equivalent (–). C: Differentials of reaction curves in (B). Absorbance changes within 1 minute are plotted from 10 to 16 minutes after the start of the reaction. Protein S activity was as follows: 0 (●), 5 (▲), 10 (■) and 15 μg/ml PS-equivalent (–). D: Calibration curve of protein S activity. The slopes of straight lines in (C) are plotted against standard protein S activity. E: Comparison of measurements of plasma protein S activity between colorimetric assay and clotting time assay.

time, as shown in Figure 1B. When the differentials of absorbance increases in a unit time are plotted against time, straight lines are obtained, as shown in Figure 1C. The calibration curve for protein S activity is obtained when the slopes of these lines are plotted against protein S concentration (Figure 1D).

Protein S activity was calculated from the calibration curve for plasma samples measured similarly. The day-to-day reproducibility was examined by five measurements of the plasma from a healthy person and a pregnant woman. In the former plasma, the mean activity was 11.0 μg/ml PS-equivalent with a

variable coefficient of 2.7%, and in the latter, 4.3 μg/ml PS-equivalent with a variable coefficient of 7.2%.

Ten plasma samples containing different amounts of free protein S antigen were prepared, and protein S activity was measured by the new method and the conventional clotting method. These measurements showed excellent correlation ($r = 0.97$) (Figure 1E).

The method we have developed for measuring protein S activity will contribute to routine operations and standardization of protein S activity measurements as well as screening for protein S abnormalities, although the sensitivity, reproducibility and cost must be further improved. In addition, it could be applied to measurement of other blood coagulation factors.

References

1. Faioni EM. Reliable estimates of plasma protein S levels: are we getting any closer Thromb Haemost 2001;86:1139–40.
2. Persson KE, Hillarp A, Dahlbäck B. Analytical considerations for free protein S assays in protein S deficiency. Thromb Haemost 2001;86:1144–7.
3. Tsuda T, Tsuda H, Yoshimura H, Hamasaki N. Dynamic equilibrium between protein S and C4b binding protein is important for accurate determination of free protein S antigen. Clin Chem Lab Med 2002;40:563–7.
4. Persson KE, Dahlbäck B, Hillarp A. Diagnosing protein S deficiency: analytical considerations. Clin Lab 2003;49:103–10.
5. Schwarz HP, Fischer M, Hopmeier P, Batard MA, Griffin JH. Plasma protein S deficiency in familial thrombotic disease. Blood 1984;64:1297–300.
6. Comp PC, Nixon RR, Cooper MR, Esmon CT. Familial protein S deficiency is associated with recurrent thrombosis. J Clin Invest 1984;74:2082–8.
7. Comp PC, Esmon CT. Recurrent venous thromboembolism in patients with a partial deficiency of protein S. N Engl J Med 1984;311:1525–8.
8. Zöller B, He X, Dahlbäck B. Homozygous APC-resistance combined with inherited type I protein S deficiency in a young boy with severe thrombotic disease. Thromb Haemost 1995;73:743–5.
9. Faioni EM, Valsecchi C, Palla A, Taioli E, Razzari C, Mannucci PM. Free protein S deficiency is a risk factor for venous thrombosis. Thromb Haemost 1997;78:1343–6.
10. Tsuda H, Hattori S, Tanabe S, Iida H, Nakahara M, Nishioka S, et al. Screening for aetiology of thrombophilia: a high prevalence of protein S abnormality. Ann Clin Biochem 1999;36:423–32.
11. Nizzi FA Jr, Kaplan HS. Protein C and S deficiency. Semin Thromb Hemost 1999;25:265–72.
12. Makris M, Leach M, Beauchamp NJ, Daly ME, Cooper PC, Hampton KK, et al. Genetic analysis, phenotypic diagnosis, and risk of venous thrombosis in families with inherited deficiencies of protein S. Blood 2000;95:1935–41.
13. Shen MC, Lin JS, Tsay W. Protein C and protein S deficiencies are the most important risk factors associated with thrombosis in Chinese venous thrombophilic patients in Taiwan. Thromb Res 2000;99:447–52.
14. Martinelli I. Risk factors in venous thromboembolism. Thromb Haemost 2001;86:395–403.
15. Burneo JG, Elias SB, Barkley GL. Cerebral venous thrombosis due to protein S deficiency in pregnancy. Lancet 2002;359:892.
16. Borgel D, Reny JL, Fischelis D, Gandrille S, Emmerich J, Fiessinger JN, et al. Cleaved protein S (PS), total PS, free PS, and activated protein C cofactor activity as risk factors for venous thromboembolism. Clin Chem 2003;49:575–80.
17. Bakker HM, Tans G, Janssen-Claessen T, Thomassen MC, Hemker HC, Griffin JH, et al. The effect of phospholipids, calcium ions and protein S on rate constants of human factor Va inactivation by activated human protein C. Eur J Biochem 1992;208:171–8.
18. Nicolaes GA, Thomassen MC, van Oerle R, Hamulyak K, Hemker HC, Tans G, et al. A prothrombinase-based assay for detection of resistance to activated protein C. Thromb Haemost 1996;76:404–10.
19. Wolf M, Boyer-Neumann C, Martinoli JL, Leroy-Matheron C, Amiral J, Meyer D, et al. A new functional assay for human protein S activity using activated factor V as substrate. Thromb Haemost 1989;62:1144–5.
20. Bergstrom K, Egberg N. Determination of vitamin K sensitive coagulation factors in plasma: studies on three methods using synthetic chromogenic substrates. Thromb Res 1978;12:531–47.

Relation of cigarette smoking and alcohol use to colorectal adenomas by subsite: The self-defense forces health study

Kengo Toyomura,[1] Keizo Yamaguchi,[1,2] Hideki Kawamoto,[1,3] Shinji Tabata,[1,3] Eiichi Shimizu,[2] Masamichi Mineshita,[2] Shinsaku Ogawa,[3] Kyong-Yeon Lee[1] and Suminori Kono[1]

[1]Department of Preventive Medicine, Faculty of Medical Sciences, Kyushu University, 3-1-1 Maidashi, Higashi-ku, Fukuoka 812-8582; [2]Self-Defense Forces Kumamoto Hospital, 15-1 Higashihon-machi, Kumamoto 862-0902; and [3]Self-Defense Forces Fukuoka Hospital, 1-61 Kokurahigashi, Kasuga-shi 816-0826

(Received July 31, 2003/Revised November 13, 2003/Accepted November 18, 2003)

While smoking has consistently been shown to be related to increased risk of colorectal adenomas, few studies have addressed the association between smoking and site-specific colorectal adenomas. The reported association between alcohol use and colorectal adenomas has been inconsistent. We evaluated risks of adenomas at the proximal colon, distal colon, and rectum in relation to cigarette smoking and alcohol use, and their interaction. Subjects were 754 cases with histologically proven colorectal adenomas and 1547 controls with normal colonoscopy among male officials of the Self-Defense Forces (SDF) undergoing total colonoscopy at two SDF hospitals. Statistical adjustment was made for hospital, rank, body mass index, physical activity, and either smoking or alcohol drinking. Cigarette smoking was significantly associated with an increased risk of adenomas, regardless of the location of the adenomas, but the increased risk associated with smoking was more pronounced for rectal adenomas. Alcohol use was associated with moderately increased risks of distal colon and rectal adenomas, but not of proximal colon adenomas. Cigarette smoking, but not alcohol drinking, was associated with greater increases in the risk of large adenomas and of multiple adenomas across the colorectum. There was no measurable interaction of cigarette smoking and alcohol drinking on colorectal adenomas. The findings corroborate an increased risk of colorectal adenomas associated with smoking and a weak association between alcohol use and colorectal adenomas. Further studies are needed to confirm whether smoking is more strongly related to rectal adenomas, large adenomas, or multiple adenomas. (Cancer Sci 2004; 95: 72–76)

Colorectal adenomas are known to be a precursor lesion of colorectal cancer,[1,2] and it has been suggested that colorectal cancer and adenomas generally share common etiological factors, with a few exceptions.[3,4] While the association between smoking and colorectal cancer is controversial, smoking has consistently been shown to be associated with increased risk of colon or colorectal adenomas.[5] On the other hand, a meta-analysis indicated that alcohol use was associated with a modest increase in the risk of colorectal cancer,[6] but the reported relation between alcohol and colorectal adenomas is rather inconsistent. Of 13 studies examining the association between alcohol use and colorectal adenomas,[7–19] eight studies suggested an increased risk of colon or colorectal adenomas associated with alcohol use,[7–14] and five studies reported a null association between alcohol consumption and colorectal adenomas.[15–19]

It has been suggested that different etiological factors may be involved in carcinogenesis at different sites of the colorectum.[3] For instance, genetic alterations differed in proximal and distal colon cancer.[20] Higher proportions of proximal colon cancer to distal colon cancer and a lower incidence of rectal cancer were observed in women, and there was less variation between high risk and low risk areas in proximal colon cancer and in rectal cancer than in distal colon cancer.[21] Not many studies have examined the association of cigarette smoking and alcohol use with adenomas at different sites of the colorectum.[17,18,22,23] Further, few studies have addressed the interaction of these two factors in the occurrence of colorectal adenomas or cancer.[9,11,12,24,25] In this study, we addressed the relation of cigarette smoking and alcohol use to colorectal adenomas by location of adenoma and their interaction in a population of middle-aged Japanese men. We also examined the association with smoking and alcohol use according to the size and multiplicity of adenomas.

Materials and Methods

Subjects. Study subjects were male officials in the Self-Defense Forces (SDF) who received a preretirement health examination at the SDF Fukuoka and Kumamoto Hospitals from January 1995 to March 2002. The preretirement health examination is a nationwide program offering a comprehensive medical examination to those retiring from the SDF. Details of the preretirement health examination have been described elsewhere.[16,23] The present study included 754 cases of histologically confirmed colorectal adenomas and 1547 controls of normal colonoscopy among 3550 men completing total colonoscopy in a consecutive series of 4209 men; 126 men refused colonoscopy; 11 men had a poor study; and 522 had partial colonoscopy. We excluded 321 men with a history of colectomy (n=20), colorectal polypectomy (n=276), or malignant neoplasms (n=25), and colonoscopic findings of the remaining 3229 men were classified as colorectal cancer (n=2), polyp (n=1470), inflammatory bowel disease (n=3), non-polyp benign lesion such as diverticula (n=207), and normal colonoscopy (n=1547). Of the 1470 men with colorectal polyps, 754 were found to have adenomas without *in situ* or invasive carcinoma. Of these adenomas cases, 409 (54%) had multiple adenomas. Number of adenoma cases by size (diameter of the largest adenomas) were: <5 mm 458, 5–9 mm 243, ≥10 mm 49, and unknown size 4. Cases having tubular adenoma with severe atypia (n=13), tubulovillous adenoma (n=12), or villous adenoma (n=1) accounted for 3.4%. In the analysis examining the association of cigarette smoking and alcohol use with colorectal adenomas by subsite, we excluded 125 cases who had an adenoma or adenomas at sites other than the specified site. The proximal colon included the cecum to the splenic flexure. The descending colon and sigmoid colon were defined as distal colon. The rectosigmoid junction was categorized as rectum. Numbers of cases having adenomas exclusively at the proximal

E-mail: kengot@phealth.med.kyushu-u.ac.jp

colon, distal colon, and rectum were 258, 292, and 79, respectively.

Lifestyle questionnaire. A self-administered questionnaire was used to ascertain smoking habits, alcohol consumption, and other lifestyle factors prior to colonoscopy. Smokers were defined as those who had ever smoked cigarettes daily for at least 1 year. Both current and past smokers were asked about the average number of cigarettes smoked per day and total years of smoking. Cigarette-years were calculated by multiplying the average number of cigarette per day by total years of smoking. Alcohol drinkers were defined as those having drunk alcoholic beverages at least once a week for at least 1 year. Current drinkers reported the consumption of five types of alcoholic beverages, i.e., sake, shochu, beer, whisky, and wine, on average in the past year, and their daily intake of ethanol was estimated. Cigarette smoking was classified into 0, 1–399, 400–799, and ≥800 cigarette-years. Alcohol use was categorized into never, past, and current use with consumption of <30, 30–59, or ≥60 ml of ethanol per day. Physical activity was evaluated with a metabolic equivalent (MET)-hour score, which was calculated by multiplying the time spent in recreational exercise by the MET value corresponding to each type of exercise (light 2, moderate 4, hard 6, and very hard 8). Body mass index (BMI) was calculated by dividing weight in kilograms by squared height in meters. BMI and MET-hours were categorized into four levels using quartiles in the distributions in the control group. The SDF rank was classified into low, middle, and high ranks. The questionnaire included dietary questions, but these questions were changed substantially twice during the study period. Thus dietary factors were not considered in the present analysis.

Statistical analysis. We examined the relation of smoking and drinking to colorectal adenomas in terms of odds ratio (OR) and 95% confidence interval (CI) on the basis of logistic regression analysis. Statistical adjustment was made for hospital, rank, BMI, physical activity, and either cigarette-years or daily intake of alcohol. Age was not taken into account because the age range was limited (47–59 years) and 98% were at age 51–55 years. Trend of association was tested by a logistic regression model by assigning an ordinal score to an independent variable under study. In evaluating the interaction of smoking and alcohol drinking on colorectal adenomas, the highest two categories of smoking (400–799 and ≥800) were combined, and lifelong non-drinking and the lowest level of alcohol use (<30 ml per day) were also combined because no measurable difference in the OR was observed between the two categories. Past alcohol drinkers were excluded when trend and interaction were assessed. Statistical assessment of the interaction was performed on the basis of the likelihood ratio test by adding cross-product terms of indicator variables representing smoking categories and an ordinal variable representing alcohol drinking categories. Two-sided P values less than 0.05 were regarded as statistically significant. All computations in these analyses were performed using the SAS software, version 6.12 (SAS Institute, Cary, NC).

Results

Table 1 shows the relation of cigarette smoking and alcohol use to colorectal adenomas of all sites and site-specific adenomas. There was a statistically significant positive association between cigarette smoking and colorectal adenomas. While a statistically significant dose-dependent relationship between smoking and adenoma risk was observed regardless of the location of adenomas, increased ORs of rectal adenomas associated with cigarette smoking were more marked than observed for proximal and distal colon adenomas. The association between alcohol use and colorectal adenomas was less evident, but increases in the OR of colorectal adenomas for moderate (30–59 ml per day) and high (≥60 ml per day) alcohol consumption were statistically significant. While there was no measurable association between alcohol and proximal colon adenomas, moderate increases in the OR associated with alcohol consumption were noted for distal colon and rectal adenomas. We also examined the association between different types of alcoholic beverages and adenoma risk, and found no beverage-specific association (data not shown).

We further examined the relation of cigarette smoking and alcohol use to colorectal adenomas according to size and multiplicity of adenomas (Tables 2 and 3). Overall, smoking was more strongly associated with large adenomas (≥5 mm) and with multiple adenomas. Large-adenoma cases accounted for 34% of proximal colon adenoma cases, 35% of distal colon adenoma cases, and 48% of rectal adenoma cases; and the proportions of multiple-adenoma cases in the cases of proximal colon adenomas, distal colon adenomas, and rectal adenomas were 29%, 29%, and 22%, respectively. Large adenomas were more frequent among rectal adenoma cases, but large adenomas generally showed greater increases in the OR associated with smoking across the colorectum. Likewise, a stronger associa-

Table 1. Adjusted odds ratios (OR) and 95% confidence intervals (CI) of colorectal adenomas according to cigarette smoking and alcohol use[1]

Variable	No. of controls	Colorectum		Proximal colon		Distal colon		Rectum	
		No.	OR (95% CI)	No.	OR (95% CI)	No.	OR (95% CI)	No.	OR (95% CI)
Cigarette-years[2]									
0	499	151	1.0 (referent)	59	1.0 (referent)	66	1.0 (referent)	11	1.0 (referent)
1–399	314	123	1.2 (0.9–1.6)	38	1.0 (0.6–1.5)	44	1.0 (0.7–1.5)	17	2.5 (1.1–5.4)
400–799	539	328	1.9 (1.5–2.4)	108	1.7 (1.2–2.3)	131	1.7 (1.2–2.7)	28	2.3 (1.1–4.7)
≥800	195	152	2.3 (1.7–3.1)	53	2.1 (1.4–3.2)	51	1.8 (1.2–2.7)	23	5.6 (2.6–11.9)
Trend			P=0.0001		P=0.0001		P=0.0003		P=0.0001
Alcohol (ml/d)									
Never	228	85	1.0 (referent)	36	1.0 (referent)	35	1.0 (referent)	6	1.0 (referent)
Past	53	24	1.2 (0.7–2.1)	9	1.1 (0.5–2.4)	10	1.2 (0.6–2.7)	1	0.6 (0.1–5.1)
<30[3]	460	162	1.0 (0.8–1.4)	62	1.0 (0.6–1.5)	54	0.8 (0.5–1.3)	21	1.9 (0.7–4.8)
30–59[3]	409	240	1.6 (1.2–2.2)	71	1.2 (0.7–1.8)	101	1.7 (1.1–2.6)	26	2.4 (1.0–6.1)
≥60[3]	397	243	1.6 (1.2–2.1)	80	1.3 (0.8–2.0)	92	1.5 (1.0–2.3)	25	2.3 (0.9–5.7)
Trend[4]			P=0.0001		P=0.14		P=0.002		P=0.09

1) Adjusted for rank, hospital, body mass index, physical activity, and either alcohol intake or smoking.
2) Cigarettes smoked per day multiplied by years of smoking.
3) Amount of ethanol (ml) consumed per day in current drinkers.
4) Past drinkers were excluded.